Kaunas University of Technology

Faculty of Mechanical Engineering and Design

X-ray Computed Tomography Based Evaluation of Internal Defects in Polymer Composite Materials

Master's Final Degree Project

Bandar Aliyev

Project author

Prof. Elena Jasiūnienė

Supervisor

Kaunas, 2026

Kaunas University of Technology

Faculty of Mechanical Engineering and Design

X-ray Computed Tomography Based Evaluation of Internal Defects in Polymer Composite Materials

Master's Final Degree Project

Aeronautical Engineering (6211EX024)

Bandar Aliyev

Project author

Prof. Elena Jasiūnienė

Supervisor

Prof. Artūras Keršys

Reviewer

Kaunas, 2026

Kaunas University of Technology

Faculty of Mechanical Engineering and Design

Bandar Aliyev

X-ray Computed Tomography Based Evaluation of Internal Defects in Polymer Composite Materials

Declaration of Academic Integrity

I confirm the following:

1. I have prepared the final degree project independently and honestly without any violations of the copyrights or other rights of others, following the provisions of the Law on Copyrights and Related Rights of the Republic of Lithuania, the Regulations on the Management and Transfer of Intellectual Property of Kaunas University of Technology (hereinafter – University) and the ethical requirements stipulated by the Code of Academic Ethics of the University;

2. All the data and research results provided in the final degree project are correct and obtained legally; none of the parts of this project are plagiarised from any printed or electronic sources; all the quotations and references provided in the text of the final degree project are indicated in the list of references;

3. I have not paid anyone any monetary funds for the final degree project or the parts thereof unless required by the law;

4. I understand that in the case of any discovery of the fact of dishonesty or violation of any rights of others, the academic penalties will be imposed on me under the procedure applied at the University; I will be expelled from the University and my final degree project can be submitted to the Office of the Ombudsperson for Academic Ethics and Procedures in the examination of a possible violation of academic ethics.

Bandar Aliyev

Confirmed electronically

Kaunas University of Technology

Faculty of Mechanical Engineering and Design

Task of the Master's Final Degree Project

Given to the student – Bandar Aliyev

1. Topic of the project

X-ray Computed Tomography Based Evaluation of Internal Defects in Polymer Composite Materials

(In English)

Polimerinių kompozicinių medžiagų vidinių defektų įvertinimas naudojant rentgeno kompiuterinę tomografiją

(In Lithuanian)

2. Aim and tasks of the project

Aim: to evaluate the internal defects in polymer composite materials using X-ray computed tomography (CT) and to analyse their distribution, morphology, and structural characteristics.
Tasks:
1. Analysis of previous research on filler dispersion in polymer composites using X-ray CT
2. Data acquisition and 3D image reconstruction of polymer composite samples
3. Develop and apply 3D image analysis methods to quantify filler dispersion and agglomeration.
4. Assess influence of processing parameters and filler characteristics on dispersion quality

3. Main requirements and conditions

Assess the internal defects in polymer composite materials using X-ray CT. The investigated materials consisted of six piezocomposite samples: three BTO and three rGO samples prepared under different extrusion conditions, with approximate lengths of 41 mm and 42 mm, respectively. Determine the size, distribution, and structural characteristics of internal defects, including pores and inclusions, and evaluate the structural uniformity of the composites.

4. Additional requirements and conditions for the project, report and appendices

Not applicable

Project author	Bandar Aliyev		15-02-2026
	(Name, Surname)	*(Signature)*	*(Date)*
Supervisor	Elena Jasiūnienė		15-02-2026
	(Name, Surname)	*(Signature)*	*(Date)*
Head of study field programs	Artūras Keršys		15-02-2026
	(Name, Surname)	*(Signature)*	*(Date)*

Aliyev, Bandar. X-ray Computed Tomography Based Evaluation of Internal Defects in Polymer Composite Materials. Master's Final Degree Project / supervisor Prof. Elena Jasiūnienė; Faculty of Mechanical Engineering and Design, Kaunas University of Technology.

Study field and area (study field group): Aeronautical Engineering (E14), Engineering Science.

Keywords: X-ray Computed Tomography (CT); Polymer Composite Materials; Internal Defects; Porosity Analysis; Inclusion Analysis; Filler Dispersion; VGStudio MAX.

Kaunas, 2026. 50.

Summary

This thesis describes a methodology involving X-ray computerised tomography (CT) for the evaluation of defects present inside the polymer composite materials. This research has been done in order to study the internal structures of polymer composites and find out the nature and distribution of any defects inside such materials. The rationale behind conducting this research has been derived from the consideration that defect and inhomogeneity properties of the composite can seriously affect the performance of the materials, and at the same time, two-dimensional observations can never give us a representative idea of the inner structure of the material.

The experiment part of the research consisted of six piezocomposite samples of two types: three barium titanate (BTO) samples and three reduced graphene oxide (rGO) samples produced using various extrusion parameters. The quantitative study revealed a definite decrease in the amount of internal defects when the extrusion passes were increased. As far as the BTO samples were concerned, the total amount of pores was equal to 980 in the first sample, decreased to 74 in the second sample, and then to 8 in the third sample, while the highest quantity of pores in the first sample was in diameters of 50-100 μm and 100-200 μm. In regard to the rGO samples, the total amount of inclusions decreased from 1819 in the first sample to 314 in the second sample and further to 307 in the third sample; the most considerable decrease was registered for diameters of 25-50 μm, where inclusions reduced their number from 1061 in the first sample to 197 and then to 176, respectively.Reconstructed three-dimensional CT scans were used for the research, which made it possible to look at the samples' interior structure without cutting or harming them. This allowed for comparisons of the flaws' size ranges, geographical distribution, and morphological features in addition to their quantity. The results are significant because they show how CT-based inspection may assist determine processing parameters that result in a more uniform internal structure and enhance the assessment of composite material quality. Furthermore, the analysis made it easier to see how internal flaws are dispersed throughout the whole sample volume as opposed to only in certain cross-sectional regions. This enhances the accuracy of the data and validates CT as a useful technique for assessing the interior quality of polymer composite materials.

On the whole, it was shown that the samples synthesised by extrusion at the latter conditions possessed less defect concentration and denser internal structure. As a result of investigation, it was found that the third samples were characterised by the least defect concentration and the most homogeneous internal structure among all studied samples. Therefore, it can be concluded that X-ray computed tomography can be successfully applied to three-dimensional non-destructive testing of internal defects in polymers.

Aliyev, Bandar. Polimerinių kompozicinių medžiagų vidinių defektų įvertinimas naudojant rentgeno kompiuterinę tomografiją. Magistro baigiamasis projektas / Prof. Elena Jasiūnienė; Kauno technologijos universitetas, Mechanikos inžinerijos ir dizaino fakultetas.

Studijų kryptis ir sritis (studijų krypčių grupė): Aeronautikos inžinerija (E14), Inžinerijos mokslai.

Reikšminiai žodžiai: Rentgeno kompiuterinė tomografija (KT); Polimerinės kompozitinės medžiagos; Vidiniai defektai; Porėtumo analizė; Įtraukimų analizė; Užpildo dispersija; VGStudio MAX.

Kaunas, 2026. 50 p.

Santrauka

Šiame darbe aprašoma metodika, pagrįsta X-ray computed tomography (KT), skirta defektų, esančių polimerinių kompozitų viduje, vertinimui. Šis tyrimas buvo atliktas siekiant ištirti polimerinių kompozitų vidinę struktūrą ir nustatyti tokių medžiagų viduje esančių defektų pobūdį bei pasiskirstymą. Šio tyrimo pagrindas yra tai, kad defektai ir struktūriniai netolygumai gali reikšmingai paveikti medžiagų eksploatacines savybes, o tuo pačiu metu dvimatės analizės negali suteikti reprezentatyvaus vaizdo apie vidinę medžiagos struktūrą.

Eksperimentinę tyrimo dalį sudarė šeši pjezokompozitiniai mėginiai iš dviejų tipų: trys bario titanato (BTO) mėginiai ir trys redukuoto grafeno oksido (rGO) mėginiai, pagaminti taikant skirtingus ekstruzijos parametrus. Kiekybinė analizė parodė aiškų vidinių defektų kiekio mažėjimą didėjant ekstruzijos ciklų skaičiui. Kalbant apie BTO mėginius, bendras porų skaičius sumažėjo nuo 980 pirmajame mėginyje iki 74 antrajame mėginyje ir iki 8 trečiajame mėginyje, o didžiausia porų koncentracija pirmajame mėginyje buvo 50–100 μm ir 100–200 μm skersmens intervale. Kalbant apie rGO mėginius, įtraukimų skaičius sumažėjo nuo 1819 pirmajame mėginyje iki 314 antrajame mėginyje ir iki 307 trečiajame mėginyje; didžiausias sumažėjimas buvo nustatytas 25–50 μm skersmens intervale, kur įtraukimų skaičius sumažėjo nuo 1061 pirmajame mėginyje iki atitinkamai 197 ir 176. Tyrime buvo naudojami rekonstruoti trimačiai KT vaizdai, kurie leido pažvelgti į mėginių vidinę struktūrą jų nepjaustant ir nepažeidžiant. Tai leido palyginti ne tik defektų kiekį, bet ir jų dydžio intervalus, erdvinį pasiskirstymą bei morfologines ypatybes. Rezultatai yra reikšmingi, nes jie parodo, kaip KT pagrįsta patikra gali padėti nustatyti apdorojimo parametrus, kurie lemia vienodesnę vidinę struktūrą ir pagerina kompozitinės medžiagos kokybės vertinimą.Be to, analizė leido lengviau matyti, kaip vidiniai defektai yra pasiskirstę visame mėginio tūryje, o ne tik tam tikrose skerspjūvio srityse. Tai padidina duomenų tikslumą ir patvirtina KT kaip naudingą metodą polimerinių kompozitinių medžiagų vidinei kokybei vertinti.

Apskritai nustatyta, kad mėginiai, pagaminti taikant vėlesnes ekstruzijos sąlygas, pasižymi mažesne defektų koncentracija ir tankesne vidine struktūra. Tyrimo rezultatai parodė, kad trečiasis mėginys pasižymi mažiausia defektų koncentracija ir homogeniškiausia vidine struktūra tarp visų tirtų mėginių. Todėl galima daryti išvadą, kad rentgeno kompiuterinė tomografija gali būti sėkmingai taikoma kaip trimatis neardomojo bandymo metodas vidinių defektų analizei polimeruose.

Table of contents

List of figures

List of tables

List of abbreviations and terms

Abbreviations:

CT – Computed Tomography

SEM – Scanning Electron Microscopy

TEM – Transmission Electron Microscopy

PMC – Polymer Matrix Composite

BTO – Barium Titanate

rGO – Reduced Graphene Oxide

CNT – Carbon Nanotube

SiC – Silicon Carbide

Al_2O_3 – Aluminium Oxide

$CaCO_3$ – Calcium Carbonate

$Mg(OH)_2$ – Magnesium Hydroxide

LDPE – Low-Density Polyethene

PP – Polypropylene

FBP – Filtered Back Projection

VOI – Volume of Interest

SSA – Specific Surface Area

STDEV – Standard Deviation

Introduction

Advanced polymer composite materials are commonly used in modern aircraft structures due to their high strength and stiffness-to-weight ratios. This yields the benefits of improved fuel efficiency, increased usable payload, and better overall aircraft performance. However, successful implementations are also conditioned by their intrinsic quality, as defects and non-uniform structure in the material can compromise reliability and adversely affect their behaviour in service conditions.

The characteristics of polymer composites depend not only on the type and amount of filler, but also on its uniformity within the polymer matrix. The poor dispersion would result in agglomeration, porosity, inclusions and other structural heterogeneities that generate regions of local stress concentration, blocking load transfer and decreasing the mechanical performance. Hence, from both the materials science standpoint and its relevance to aeronautical applications, accurate assessment of internal microstructure is paramount.

The standard approaches for characterising composites, namely optical microscopy and scanning electron microscopy are limited by the two-dimensional nature of their observations which fails to truly represent the internal structure of composite materials. Due to the limited nature of these techniques in looking at isolated cross-sections, they may not properly reflect the true 3D distribution of fillers and internal defects across the body of sample. As a result, significant structural attributes may go unnoticed or may be misinterpreted.

Because of this trend, three-dimensional non-destructive evaluation methods have come to play an increasingly important role. X-ray computed tomography is of particular relevance to polymer composites, as it allows non-destructive 3D imaging and quantitative analysis of pores, inclusions (large or small), agglomeration, and structural heterogeneity in voluminous samples, unlike other methods. Hence, it provides a more reflective assessment of internal structure than traditional 2D methods.In this context, the current study is specifically focused on X-ray computed tomography-based evaluation of internal defects in polymer composite materials. The work involves CT data acquisition; three-dimensional reconstruction and image-based description of structural aspects associated with filler dispersion, porosity, inclusions, and agglomeration, all in the context of composite behaviour and the effects of process conditions.

The aim of this study is to evaluate the internal defects in polymer composite materials using X-ray computed tomography (CT) and to analyse their distribution, morphology, and structural characteristics.

The following tasks were established in order to accomplish this aim:

- Analysing previous studies on filler dispersion in polymer composites using X-ray CT in order to define the theoretical background for the present study and identify relevant parameters for CT-based evaluation
- Acquiring CT data and reconstruct three-dimensional images of polymer composite samples;
- Developing and applying image analysis methods for quantifying filler dispersion and agglomeration;
- Evaluating the influence of processing parameters and filler characteristics on dispersion quality

1. Literature Review

The fillers in polymer composites are essential to their mechanical performance, but the distribution of these fillers within the matrix is a significant factor driving this. The homogeneous dispersion of fillers enhances the transfer load and mechanical robustness, contrary to forming agglomeration, which can lead to stress concentration areas with low reinforcement. Accordingly, it is important to understand and measure the filler dispersion in order to predict the behavior of composites. Filler distribution has been characterised by various means, such as conventional two-dimensional microscopy. However, such methods are limited in that they do not fully characterise the 3D microstructure of composites. In this regard, X-ray computed tomography (CT) has received significant interest as a non-destructive tool to offer 3D structural details. The current work is based on these studies mentioned above and reviews the developments related to filler dispersion, its role in mechanical properties, and the CT-based techniques for quantitative microstructural analysis in this chapter.

1.1. Polymer Composites and the Role of Fillers

Polymer composite materials can be described as a combination of materials that include a polymer matrix and a reinforcement component either in particle or fiber form. The reinforcement component helps in achieving improved mechanical properties such as increased strength and stiffness. The matrix is essential in binding together the reinforcement, transferring loads to them, and shielding them from environmental impacts. Consequently, both reinforcement and matrix are very critical in deciding the final response of polymer composites [1].

Polymers matrix composites (PMCs) are constantly used for many engineering purposes because of their high specific strength, corrosion resistance, low density, and fabricability. PMCs are also cheaper to manufacture and easier to design than CMCs or MMCs. Brick and Iwatsubo found that PMCs are both cheaper to manufacture and easier to design than CMCs or MMCs. Due to these properties, PMCs are important types of composite materials for engineering applications. [1].

Fillers are incorporated into polymers to reduce costs and improve their physical, chemical, thermal, and electrical properties. Since fillers usually act as load reducers, it has been shown that the addition of inorganic fillers such as SiC, Al2O3, CaCO3, and Mg(OH)2 can have a ripple effect on the tensile strength of composites, as these phenomena are considered. Therefore, when we add fillers, we not only change the material's price but also its physical characteristics. For this reason, fillers play a significant role in polymer composite design [2].

The effectiveness of fillers depends on particle size, loading fraction, dispersion homogeneity, and crack-bridging force at the filler-polymer interface. Uniform dispersion of fillers enhances the stress transfer from the matrix to the filler particles. On the contrary, nonhomogeneity or agglomeration is likely to lead to stress concentration and mechanical degradation. Hence, filler dispersion has an immediate impact on the mechanical properties of polymer composites [2].

With the introduction of thermoset composite wastes, in addition to conventional fillers, as alternative filler materials in polymer composites, GFRP (Glass fiber reinforced polymer) wastes are of significance in this context, as their disposal by incineration or landfilling can generate adverse environmental impacts and high costs. For this reason, their re-utilisation as filler materials is regarded as a useful approach. Other studies have already demonstrated a positive effect of thermoset

waste fillers on the flexural and compressive behaviour of polymer mortar, especially with coarse waste particles or when silane coupling agents are used [3].

1.1.1. Effect of Fillers in Polymer Composites and Mechanical Behaviour of Particulate Systems

The addition of fillers to a polymeric base significantly alters mechanical and functional response of the composite systems. Although there is historical precedence to introduce fillers to lower cost, in current composite technology, they act as means for adjusting stiffness, dimensional stability (decreasing risk of distortion), thermal resistance, and structural performance (Wypych, 2016; DeArmitt & Rothon, 2017). The filling agents are thus not only imparting bulk strength but actively influencing atomistic- and interfacial-level phenomena [4,5].

When introducing particulate fillers into polymers, the modulus of the polymer is generally increased as a result of the higher intrinsic stiffness of fillers relative to that of the matrix. This reinforcement of stiffness is frequently observed even at relatively low levels of filler loading. However, improvements in tensile and slipping resistance are not always directly achieved and depend significantly on the characteristics of a filler as well as the architecture of the composite (DeArmitt & Rothon, 2017). To give an example that shows the relationship between matrix properties and mechanical response of filled composites, shown in Fig. 1 Throughout many systems, elevating filler loading transitions to enhanced stiffness and diminished ductility is achieved due to restraining polymer chain mobility and creating stress concentrations adjacent to stiff inclusions [5].

Particle-filled polymers are influenced by several reciprocal variables, such as particle size, shape, and surface area concentration, degree of filling, and bulk properties of the polymeric matrix. Also, direct effects of a similar filler on reinforcing behaviour could be different due to matrix stiffness and its dependence on deformation (reinforcement efficiency is a property of the matrix [4].

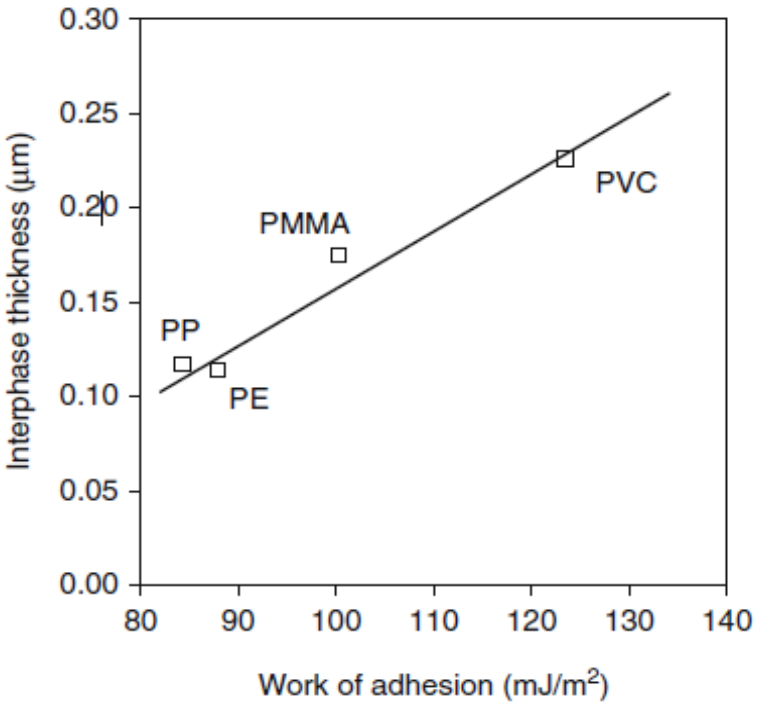

Fig. 1. Dependence of tensile yield stress on matrix properties in $CaCO_3$-filled composites

The adhesion between a filler and matrix is extremely important to the stress carryover from the matrix to the fillers. The increase in bonding capacity binds better load transfer and restrains debonding, but a poor interface adhesion can create voids and even" premature crack. Surface modification and interfacial adhesion are essential for improved mechanical properties [4]. Additionally, polymer-particle interactions that occur during processing can produce an interphase with dissimilar properties to the bulk polymer, which also influences deformation response.

In addition to the filler content, the morphology of fillers and their contact behaviour can also have an influence on compositing. Interfacial properties and microstructural design can be tuned to an extent such that functional responses are enhanced remarkably, showing the importance of morphological effects directly or indirectly through filler distribution to overall macroscopic behaviour [6].

In general, fillers affect polymer composites by a combination of stiffness contrast, interfacial interaction, particle geometry, and structure organisation. Consequently, both the filler type and content, as well as the microstructural organisation, must be known to establish meaningful structure–property relations for particulate-filled polymers [4,6].

1.1.2. Influence of Filler Volume Fraction, Particle Size, and Micromechanical Reinforcement Mechanisms

Mechanical behaviour of filled polymer composites strongly depends on the filler volume fraction, and it usually increases with increasing rigid particle content due to higher modulus values of inorganic fillers in comparison with the matrix. This stiffening is due to the action of fillers in restraining matrix flow and acting as a load-bearing material, allowing some applied stress to be transferred from the polymer fraction to the reinforcing fraction [7, 8].

But the mechanical properties do not always rise with the filler content increasing, for too much loading can lead to abrasive particles and agglomerates as well as stress concentration within the composites. The particle size is also an important parameter that affects the reinforcement efficiency, with smaller particles offering a larger interfacial area and hence leading to better stress transfer as well as mechanical property improvement, provided that dispersion is homogeneous [7].

On the other hand, larger particles or agglomerates can act as local defects in the substrate upon sintering, giving rise to localised stress fields that favour crack initiation and lower strength and fracture resistance [7].

The composite mechanical properties of particulate composites can be predicted by mm models, such as the rule of mixtures, in which the stiffness ,for example, composite modulus, is simply proportional to volume-weighted contributions from matrix and filler. However, the true reinforcement efficiency arises highly from interfacial adhesion and filler dispersion, as poor bonding or inhomogeneous dispersion hinders the effective transfer of stress [8].

In addition, fillers change the local stress distribution in the polymer matrix, and insufficient interface bonding between fillers or inhomogeneous dispersion can lead to areas of higher stress concentration that favour debonding between particle and matrix and crack initiation from the particle under mechanical stresses. In contrast, fillers well dispersed in the matrix with good interfacial adhesion increase the stress transferring capability and channel of energy dissipation, and thus improve fracture

toughness by changing the cracking mode as well as consuming energy during crack propagation. Hence, the filler volume fraction, particle size, interfacial connection, and dispersion quality are the factors that synergistically influence the reinforcement performance and bulk mechanical properties of particulate polymer composites through controlling stress transfer retention behaviour and structure integrity [9].

1.2. Effect of Filler Dispersion and Agglomeration on Mechanical Properties

The mechanical performance of particulate polymer composites is greatly affected by the dispersion of fillers, because non-homogeneous distributions result in structural heterogeneities which induce localised stress concentration when subjected to external loading. These stress concentration zones trigger micro-mechanical processes such as particle debonding and crack formation, which control the deformation and failure of the composite. Aggregates decrease both the strength and fracture resistance of composites as the aggregated particles behave as points of crack initiation and serve to grow the cracks Fig. 2 and Fig. 3 [10].

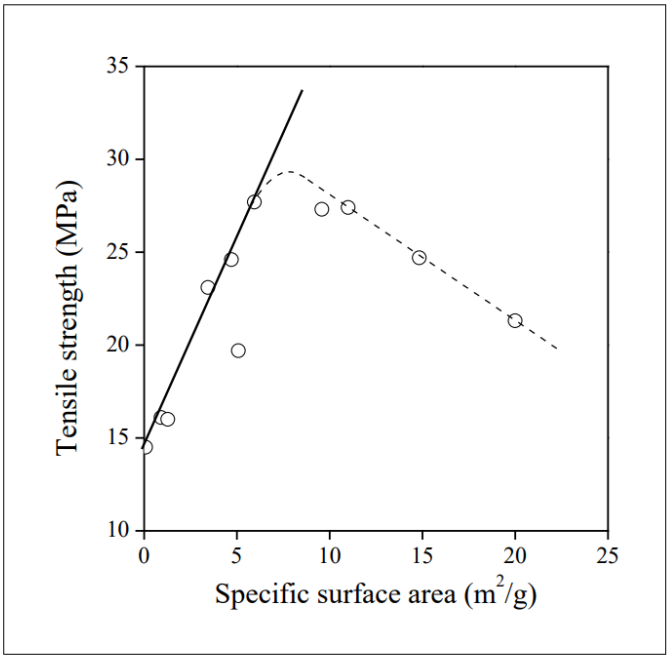

Fig. 2. Dependence of composite strength and fracture resistance on filler specific surface area, illustrating the negative effect of particle aggregation

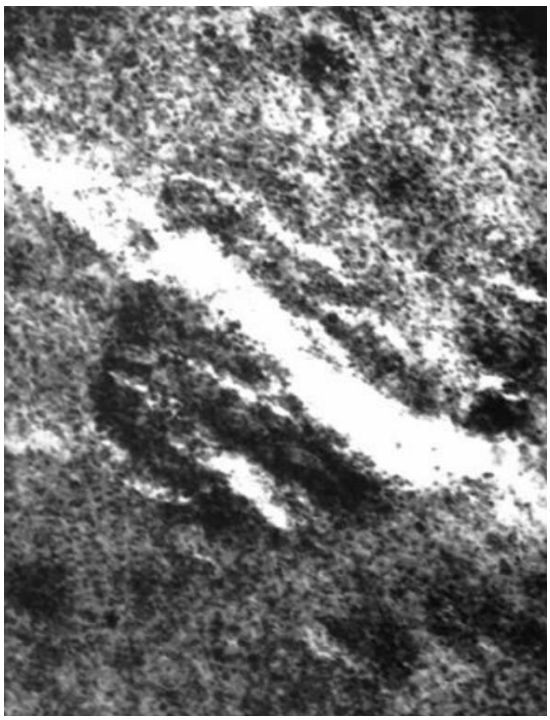

Fig. 3. Crack initiation and propagation through an aggregate in a PP/$CaCO_3$ composite, demonstrating aggregates acting as fracture initiation sites

Conversely, when fillers are uniformly dispersed, stress is transferred more efficiently from the matrix to the filler, which enhances mechanical properties and decreases points of stress concentration. Thus, the dispersion of the fillers is a prime factor that controls the strength and fracture behaviour in general and the mechanical performance reliability in particular of PP composites [10].

1.2.1. Effect of Agglomeration on Stress Concentration in Polymer Composites

A combination of single filler particles forms agglomerates, which leads to an inhomogeneous dispersion within the polymer phase that forms structural non-uniformities serving as defects and trigger stress focusing upon mechanical loading. It is observed that such agglomerations diminish the effective interfacial surface area of filler to polymer, and thus a relatively low efficiency for stress transfer, which weakens the reinforcing effect of fillers [11]. Thus, the stress is normalised around agglomerates, and it does not distribute in a uniform pattern, which allows for crack starting followed by structural failure. Aggregates also inhibit molecular mobility, generate interface defects which cause more local stress, and cause cracks to be more effectively spread through grouped particle areas [12]. Furthermore, agglomerated nanoparticles serve as dispersion phases in composite material, which induce regions with poor mechanical performance and leads to sharp decrease of Young's modulus compared with that for composites using uniformly distributed fillers [11].

Schematic representations of these areas, as well as the potential effect of particle clustering on stress distribution and a reduction in the effectiveness of reinforcement, are illustrated in Fig. 4 and Fig. 5, respectively [12].

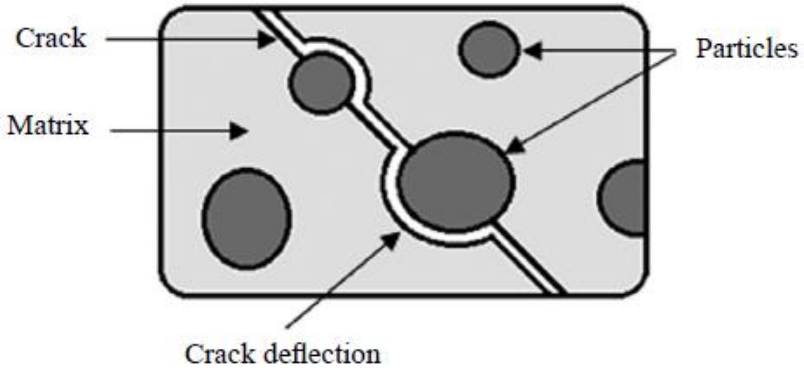

Fig. 4. Schematic illustration of filler–matrix interphase and stress transfer regions in particulate composites

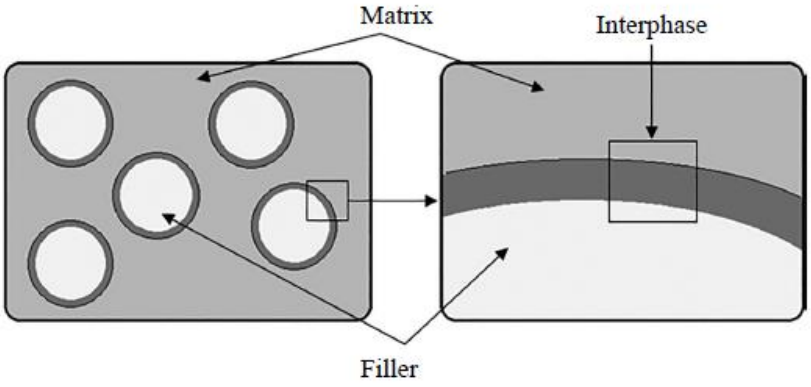

Fig. 5. Schematic representation of the filler–matrix interface structure

Similarly, Fig. 6 and Fig. 7 between the volume fraction of filler particles and the mechanical properties are indicative of the existence of aggregation/agglomeration processes and their effect in reducing composite modulus by inducing stress concentration [12]. As a result, fillers could get together when that occurs, and mechanical adverse effects like the contact point of the stress between parts, decreasing effectiveness in transferring load, and even lowering the integrity of the whole composite substances and compounds can be observed [13].

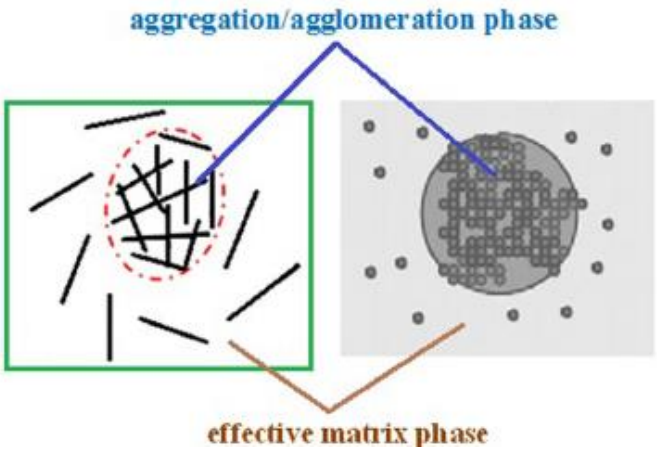

Fig. 6. Schematic representation of aggregation/agglomeration regions and effective matrix phase in polymer nanocomposites containing dispersed and clustered nanoparticles

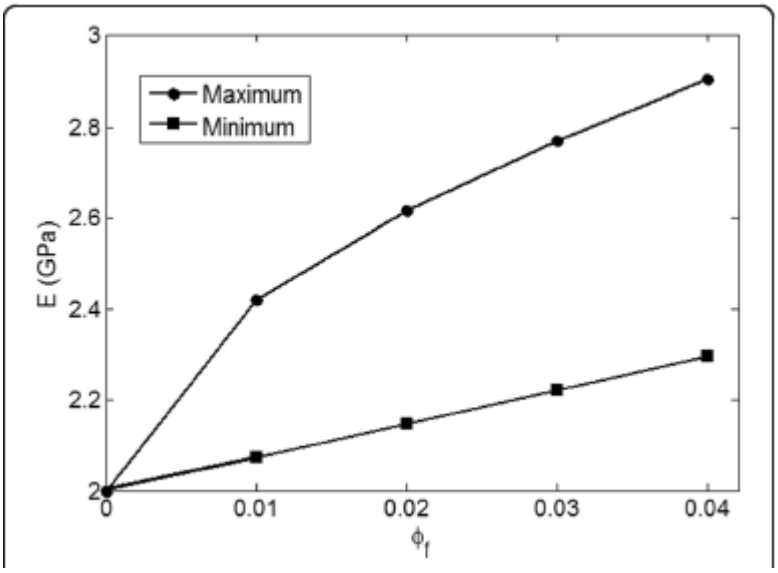

Fig. 7. Maximum and minimum predicted Young's modulus of polymer nanocomposites as a function of filler volume fraction, illustrating the influence of nanoparticle aggregation/agglomeration

1.2.2. Particle Clustering Tensile Strength Composite

The tensile strength of PPCs is significantly influenced by the spatial distribution of reinforcing particles; uniform dispersion leads to an effective stress transfer from matrix to fillers so that fillers can effectively participate in bearing load and strengthening. When fillers clump together, they form clusters instead of spreading evenly throughout the matrix. This weakens the reinforcement, as these particles do not effectively transfer loads. As a result, the overall strengthening effect in composites is reduced [14]. Particle agglomeration also forms concentrated zones of stress localisation, thus promoting particle cracking and premature damage initiation under tensile loading, resulting in deteriorated tensile strength [13]. The mechanical simulations and experimental results demonstrate that the clustered micro-structures have many more broken particles than the uniformly dispersed ones, leading to low flow stress, low tensile strength, and poor mechanical reliability [13]. Experiments also show that tensile strength improves with increasing percentage of fillers only up to a critical filler loading, after which particle coagulation increasingly influences performance and impairs strength because of inefficient load transfer and the generation of structural defects [15]. Clustering causes a loss of reinforcing action, diminishing the interface bonding between fillers and matrix (with reduced stress transfer efficiencies), which further initiates early damage and crack formation in the clusters [16]. Instead, the stretching response is enhanced when particles are better distributed because they can still achieve effective load transfer and delay damage onset, while one or both reinforcing mechanisms effectively work to improve tensile performance [14, 17]. Consequently, particle clustering is harmful to tensile strength as it lowers effective reinforcement efficiency and increases stress concentration, breaking primary particles, leading to more damage evolution and hence weakening the mechanical properties of the particulate polymer composites.

1.3. Characterisation of Filler Dispersion 2D vs 3D Approaches

Traditionally, evaluation of filler dispersion and agglomeration in polymer composites is carried out through 2D imaging methods like scanning electron microscopy (SEM), optical microscopy, and transmission electron microscopy (TEM) that provide spatial visualisation of dispersed segments of fillers or aggregates in the matrix. Through SEM, we obtain micrographs that can be further digitally

analysed (e.g., through binary conversion and spatial analysis) to discriminate filler areas from matrix ones and to assess the dispersion homogeneity according to the particle distribution itself. Fig. 8-9 show some examples for SEM based dispersion analysis and image-processing techniques used for the quantitative evaluation of filler dispersion. Optical microscopy and its derivatives have been widely used to evaluate the presence of larger agglomerates and structural heterogeneities, but they do not provide sufficient resolution or field of view to fully analyse nanoscale dispersions [18]. For the quantification of filler dispersibility from 2D micrograph images, one is faced with the challenge of identifying the discrete transparent particle and computing relevant properties such as its density, location, and orientation while confronting an inhomogeneity in contrast among particles intermingled in a structure when it comes to overlapping [19].

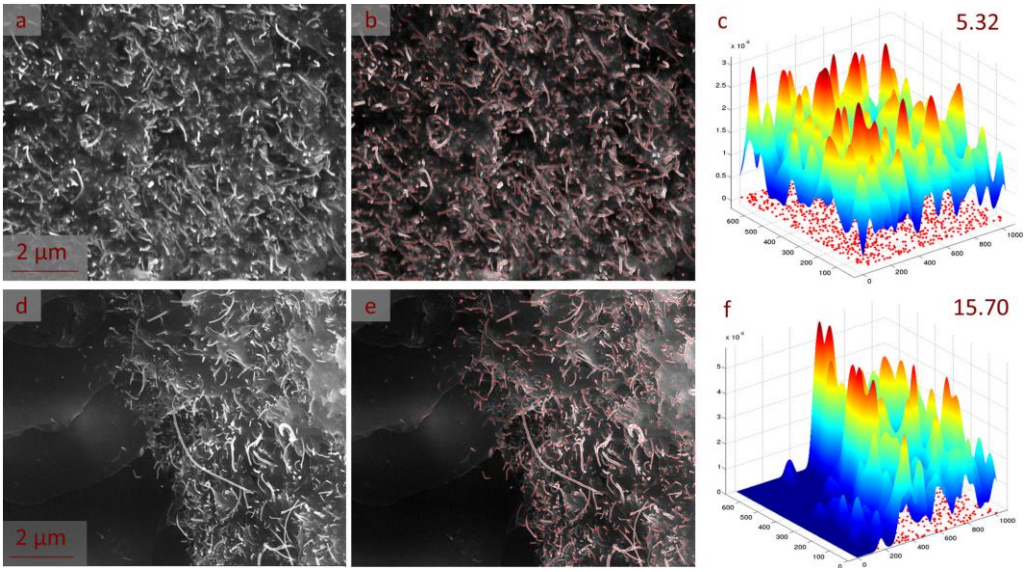

Fig. 8. Quantitative characterisation of filler dispersion showing well-dispersed and agglomerated CNT distributions and corresponding dispersion index evaluation

More sophisticated image analysis techniques (thresholding, shape recognition algorithms) can discriminate fillers and calculate dispersion-related parameters such as dispersion indices and orientation features [19].

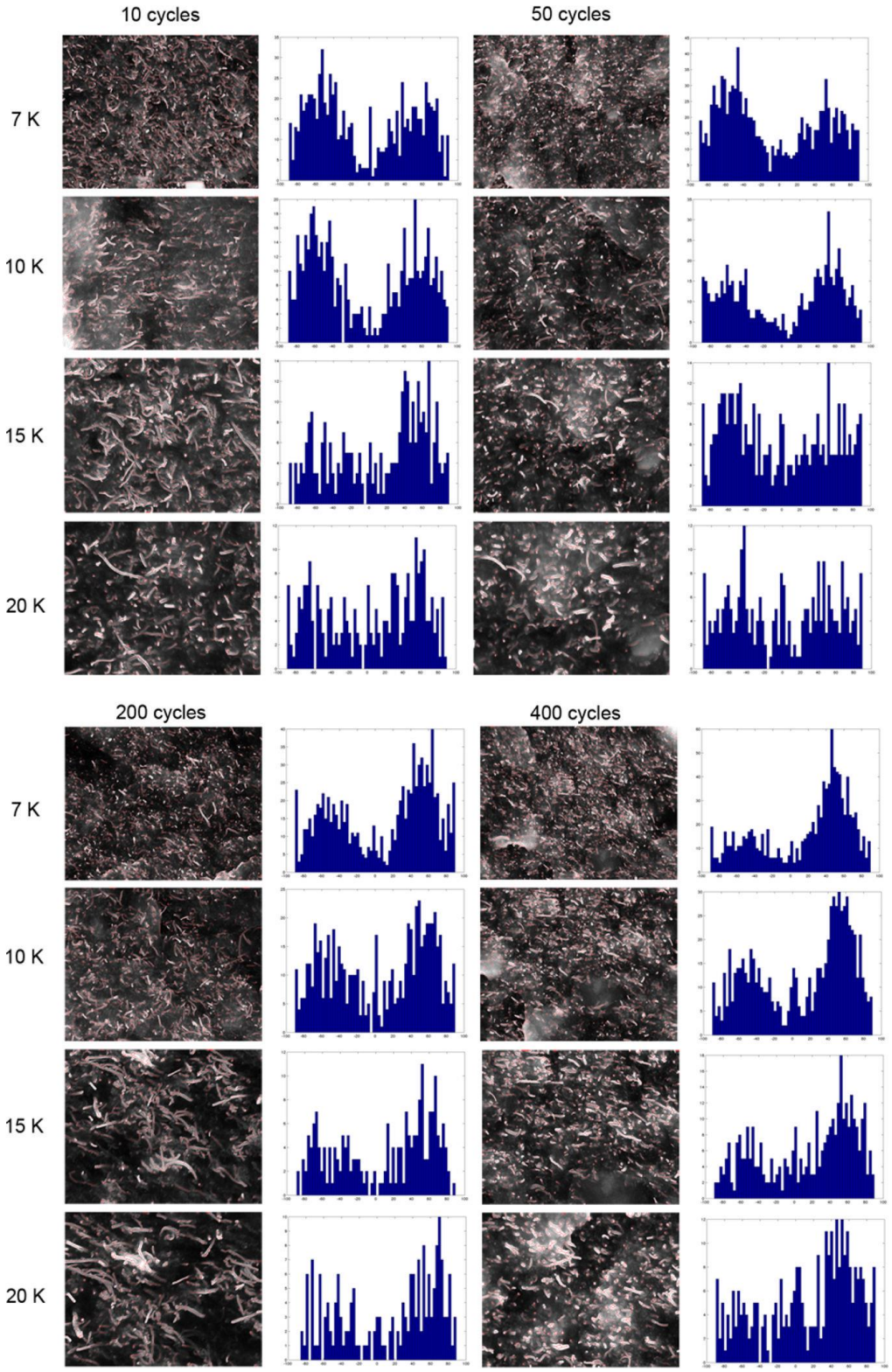

Fig. 9. SEM image of CNT-reinforced polymer composite and automatic identification of nanotubes using image processing for quantitative dispersion analysis

Although of obvious utility, 2D techniques are inherently limited in their analysis as they evaluate a single cross-sectional plane that represents a localised volume within the composite rather than the entire composite volume. To confine the microstructure of the observed sample to a thin section, for instance by a TEM study, implies that only a small part of the material is considered, which may in general not be typical for all filling distributions [18]. Also, surface characterisation techniques such

as Raman mapping inform only about the surface dispersion, and this might not reflect how well distributed fillers are inside the bulk material [20]. Such limited volume effects would consequently give rise to the representative volume problem (RVP), where a given analysed region cannot be representative of an entire microstructure's dispersion [18, 20]. Besides, 2D projection images do not adequately represent the realistic three-dimensional morphology and connectivity of fillers as well as their spatial arrangements (unlike in the case of SEM or TEM observations). This may lead to an incomplete or even misleading interpretation of dispersion conditions [20]. Three-dimensional (3D) characterisation techniques have been devised to overcome these limitations, in which the image data was collected at different depths and based on which the internal of the composite is reconstructed for volumetric estimation of filler distribution [21]. This three-dimensional methodology allows for a more precise characterisation of filler dispersion, agglomeration, and spatial distribution through the material without potential pitfalls arising from sectioning and projection errors [20, 21]. An equally large benefit of 3D characterisation is that it fosters statistically representative results by the analysis of larger volumes of a material, which adds to the reliability of quantitative dispersion values [18]. Thus, 2D imaging techniques only reveal qualitative and limited quantitative information, which is barely sufficient to obtain an accurate, representative, and reliable overview of filler dispersion in polymer composites [19].

1.3.1. SEM Analysis Filler Dispersion Limitations

The SEM-based dispersion evaluation is often carried out on 2D cross-sectional micrographs that consider fillers as "objects," and then, the quantitative measures (e.g., orientation, size/area–length distribution, local density) are obtained using digital image analysis . An example workflow process is pre-processing → segmentation → measurement, where removal of noise (Gaussian filtering), separation of fillers from the background (thresholding/segmentation), and morphology-based tools are utilised to calculate distributions: e.g., structure tensor for orientation, granulometry for size/length, or filtered imaging to create density heat maps. However, segmentation is still a major drawback of 2D SEM analysis, as automatic thresholding approaches can lead to over-segmentation and therefore unreliable particle statistics, shown in Fig.10 [22].

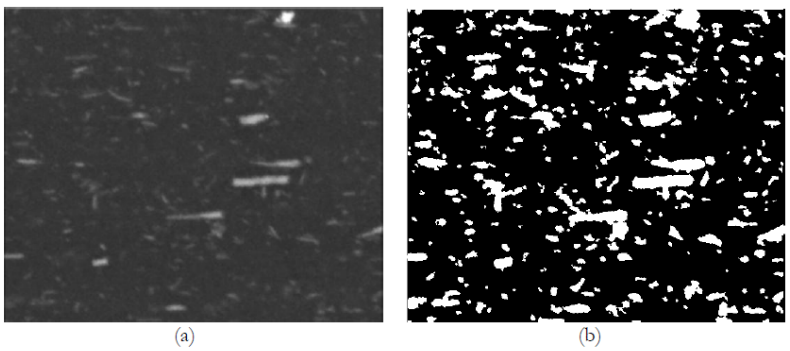

Fig. 10. Example showing how an automatic thresholding approach can over-segment a SEM image, demonstrating a key limitation of 2D SEM-based dispersion quantification

Moreover, SEM images may include acquisition artefacts (e.g., shadows/blobs) which produce "false objects" after pre-processing and directly pollute dispersion measures if not corrected [22]. Sectioning error (2D slicing bias) results from the analysis of a single cross-sectional plane of a three-dimensional particle system; consequently, filler particles may only be observed partially or may not

be found at all as they might not be sectioned by the which can result in inaccurate estimation of particle size, density, and dispersion [23].

This bias is worse in thicker sections, or when particles are thickly packed: profile contacts and axial deformations affect the correctness of particle identification, and distort area and volume estimations made from 2D images [23]. Representative volume problem: 2D imaging usually only looks at a small field of view; if you zoom in to see things better, you could be analysing such a small part of the material that it no longer represents the overall material, and your measured "dispersion" will become statistically meaningless. More generally, numerous microstructural characteristics (and curiosities) cannot be trustworthily quantified from a single (or few) 2D random cross-sections, and hence something that is statistically representative of a volume is essential in order to make claims about dispersion quality [24].

Two-dimensional analyses fail to account for the inherently three-dimensional nature of other features, such as particle connection, cluster shape, and the spatial arrangement of fillers. In practice, one could realise 3D dispersions using a volumetric method (e.g., micro-CT), but this is generally limited to maintaining realistic micrometre-range sample sizes and only affords partial/planar analysis, which could lack practical value [25].

1.3.2. 3D Microstructure Characterisation of Polymer Composites

2D characterisation techniques such as SEM, optical microscopy, and similar image-based methods are commonly employed to inspect the dispersion of fillers owing to their real-space visual capabilities, and they can unveil characteristics such as filler distribution, matrix–reinforcement adhesion, and morphology in general with high image resolution. However, the accuracy of 2D results is questionable when quantitative evaluation of dispersion is the goal to hit, since typically microscopy measures by its nature only a few enough grain boundary segments (small "field of view"), potentially diminishing the "statistical correctness" in measurements, at least where generalising to the whole bulk material [26]. This limitation is further revealed when the imaged region does not contain a sufficient number of inclusions to overestimate the microstructure-content: on one segmentated slice, predictions based on morphology information deviated more for the low-volume-fraction case (a fact explicitly attributed by its authors because there were few particles on that slice, making it non-representative by itself). Agreement increased when data from two segmented slices were incorporated in the same analysis set, indicating that there is an opportunity to improve representativeness with increased sampling even within a 2D-oriented paradigm. The same study notes that such a "few slices may be enough" for sampling. This was probably because the reinforcement was isotropic (spherical); however, the finding, combined with one, suggests that for real composite systems with more complex, anisotropic or clustered filler morphologies, 2D sampling is even more likely to miss the true spatial distribution of the 3D population. Thus, the principal reason why 2D analysis fails to describe a true 3D dispersion is that it only samples a planar portion of a full/volumetric structure; naturally, the measured dispersion status highly relies on whether the section(s) specifically chosen are statistically adequate to represent the whole volume under investigation. This raises the methodological requirement of volumetric (3D) microstructure characterisation, or at least a suitable multislice sampling strategy, in order that statements about dispersion quality are based on representative microstructural information rather than potentially biased single view [27].

1.4. Principles and Applications of X-ray Computed Tomography (CT) in Polymer Composites

X-ray computed tomography (CT) is a non-destructive imaging technique that can elucidate the internal three-dimensional structure of a sample by reconstructing an object from several two-dimensional projection images taken from multiple positions at different angles of rotation around the object Fig. 11 [28].

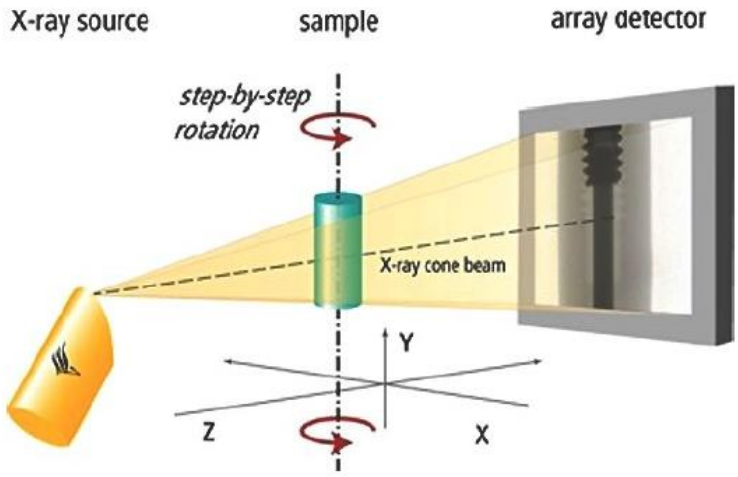

Fig. 11. Schematic of an X-ray computed tomography system showing projection acquisition and 3D reconstruction process

The basic concept on which CT imaging is based lies in the X-ray attenuation through a material; as a blast of radiation penetrates the subject, transmitted intensity attenuates according to density, atomic number, and thickness. Attenuation is governed by an exponential relationship, where the amount of transmitted X-ray intensity is proportional to a given linear attenuation coefficient for a specific material; a parameter in which both material density and atomic number, as well as X-ray energy, contribute [29]. Contrast in the projections, due to the absorption of X-rays by different components of a material, can be exploited to detect features such as fibres (or voids) and matrix (or defects) together with their distribution within the material [30]. The 3D volumetric representation of the scanned object was reconstructed from several 2D projections through mathematical reconstruction algorithms. One method that is widely used in reconstruction is FBP (filtered back-projection), a method that reconstructs the internal structure by repeating mathematical projection and filtering of the attenuation data from various angles. Other reconstruction methods, such as the iterative method, have been used to obtain a more accurate image and a lower amount of image artefact and reconstruction error. However, there may be constraints on reconstruction accuracy, such as the finite number of projections and the presence of physical artefacts that can corrupt the reconstructed image [29].

The CT volume image generated is composed of voxels as the smallest unit in a 3D dataset. In the resulting image, each voxel has a grey-scale value, representative of the bulk attenuation coefficient at that location in the specimen, and can be used to distinguish between phases in the composite. The voxel size is an important parameter in CT imaging, and is generally fixed to the field of view divided by the number of detector pixels. The spatial resolution in CT is not determined solely by the voxel size, but also by a number of system parameters, such as the detector properties (such as pixel size),

system magnification, and the X-ray source properties. Practically, however, in order to ensure robust detection of structural features, the size of the feature should go beyond single voxels, as single voxels themselves do not carry a substantial amount of spatial contrast [31].

X-ray CT is one of the radiation-based, non-destructive 3D imaging techniques that visualise the internal structure without any physical change or damage to a target [28]. Such an ability allows for detailed analysis of near-projected and projected internal features such as voids, cracks, fibre orientation, fibre architecture, and damage mechanisms in polymer composites. The multi-scale visualisation is also possible due to the CT imaging, facilitating structural identification at a component and fibre level. It can also be utilised for tracking structural changes over time and observing damage evolution during mechanical loading via in situ or time-lapse imaging methods [29]. It has some drawbacks, however, that still need to be addressed for X-ray CT. One of the main drawbacks to these technologies is the compromise between spatial resolution and field of view, because higher resolution imaging generally seeks smaller sample sizes [31].

Image resolution also depends on the contrast sensitivity, which value is determined by the attenuation differences of material phases. The low contrast between the formative polymer matrix and fibres can limit feature detectability [30]. Noise, which can also disrupt the image quality and quantitative analysis, as well as segmentation, is another challenge [31].

In general, X-ray CT is presented as a powerful and flexible technique for nondestructive 3D characterisation of polymer composites, allowing detailed imaging and quantitative analysis of their internal microstructure [30]. Nonetheless, reliable and accurate results depend on the consideration of imaging parameters, resolution restrictions, and likely artefacts in data acquisition and analysis [31].

1.4.1. X-ray Computed Tomography Filler Distribution

Recent advances in X-ray computed tomography have made it possible to observe the internal structure of polymer composites and thus investigate the spatial distribution of reinforcing components and voids without sample destruction [30]. The method is based on differences in X-ray attenuation for composite constituents (e.g., filler particles, fibres, and matrix) that give rise to contrast in the reconstructed volumetric data, enabling them to be discriminated [32]. In this manner, reconstructed CT datasets are very dense = voxel-based representations where each voxel holds information on its material properties locally, therefore providing the possibility of filler tracking within the composite volume [33]. This feature enables us to study the spatial distribution and inhomogeneity of reinforcing phases – important parameters that strongly govern the mechanical properties of composite materials [34].

In addition, it is possible to investigate structure features on several length levels from the general component geometry to single reinforcing elements using CT imaging [30]. Apart from the qualitative visualisation, CT data can also be utilised for quantitative characterisations of composite microstructure (e.g., image processing and segmentation) of the reconstructed voxel data. This allows determination of important structural parameters like the volume fraction, spatial distribution, and morphology of the reinforcing phase that are needed in order to evaluate performance [33].

X-ray computed tomography (CT) can effectively reveal the filler distribution and internal structure of polymer composite; this serves as a basis for quantitative analysis of dispersion in the follow-up study [34].

1.4.2. CT Imaging Principles, Materials Science, and Limitations (Noise, Artifacts, Contrast, Resolution Limits)

Despite its impressive benefits, X-ray computed tomography has a few drawbacks which might compromise the quality of a reconstructed image and the precision of microstructure analysis [35]. One of the main limiting factors is image noise, i.e., random variations in grey level, which can affect the sharpness and contrast of an image. The noise typically arises from effects such as X-ray scatter, finite number of projections, and detector sensitivity, which may interfere with the ability to detect weak structural features when they are small. Ring artifacts can be another effect in reconstructed images caused by deficiencies in the detector or mis-calibration. These artifacts create non-real structural patterns and can be an obstacle to the correct interpretation of material microstructure. A further disadvantage is the low contrast between distinct material phases, which becomes an issue if the attenuation differences of filler and matrix are small [32]. The poor contrast impedes the differentiation of each phase and lowers the accuracy of segmentation and quantification. Thus, noise, artefacts, and contrast limitations must be carefully accounted for to achieve valid microstructural characterisation of composites, even when X-ray CT's superior ability to yield 3D signal is taken into account [36].

1.4.3. How Computed Tomography has been used for Quantitative Evaluation of Filler Dispersion

The unprecedented non-destructive veracity of X-ray computed tomography (CT)—which uses projections to reconstruct the internal 3D morphology of heterogeneous materials without sectioning, taking away projection bias is a new device used for quantification of filler distribution in polymer composites [35].

CT does not face the drawbacks of 2D microscopy, enabling direct visualisation and quantification of agglomerates, clusters, and network connectivity in a true three-dimensional representative volume that is indispensable to discerning stress transfer pathways and defect populations in particulate and fibre-reinforced systems [35].

CT, in dispersion studies, plays the role of a quantitative metrological tool with voxel-based reconstructions manipulated to obtain morphometric and topological descriptors related to mechanical performance, instead of exclusively considering visual analysis data [37].

Image Acquisition and Resolution Considerations

Dispersion quality and reliability quantification begin at the maturity acquisition stage—determining spatial resolution, contrast, and controlling for artefacts as root determinants of reconstructed microstructure fidelity [35].

CT reconstruction algorithms (for example, Feldkamp for cone-beam geometries) construct a voxelised 3D attenuation map of the sample from the projection data. However, for quantitative interpretation, careful tuning of scanning parameters is required because beam hardening, noise, and

poor phase contrast may affect low-value distributions with possible detrimental impact on the quality of segmentations, according to research by E. Maire & P. J. Withers [35].

Micro-CT and Multiscale Imaging for Filler Dispersion Analysis

Ferreira demonstrated that cellulose fibre agglomeration in LDPE composites can be identified and quantified using micro-CT imaging. Additionally, it showed that applying the same segmentation conditions to all samples is necessary for differences in calculated dispersion parameters to reflect actual variations between materials rather than changes introduced during image processing [37].

Penumadu et al. showed that micro-focus X-ray computed tomography can be applied to the 3D localisation and characterisation of filler particles like sulphur and ZnO in rubber composites. They show the potential of XCT being a non-invasive method that allows analysing the internal particle distribution in heterogeneous polymer systems without cavitation on the structure of the material [38].

Li et al. demonstrated that the filler dispersion behaviour in polymer composites often must be evaluated over several length scales. The study illustrates the value of multiscale three-dimensional structural analysis through the combination of synchrotron CT, which provides submicron-scale insight into three-dimensional structures, and 3D-STEM imaging, which reveals nanoscale features, showing that agglomerates can play a role in determining how larger structural networks develop in the material [39].

1.4.4. Segmentation: The Dominant Source of Quantitative Uncertainty

Segmentation is the single most important step in CT-based dispersion analysis, since all morphological and topological descriptors are extracted from the binarised filler phase, so any misclassification at this stage propagates as a quantitative error throughout the analysis [35].

Variations in grey-value within CT volumes may be caused not only by material contrast but also by beam hardening, ring artefacts, noise, and polychromatic source effects, so naïve thresholding can yield physically incorrect filler volumes or artificially merged/split clusters [35].

More clearly can be said if we select thresholding improperly :

1. Clusters may artificially merge
2. Large agglomerates may fragment
3. Volume fractions may be over- or under-estimated
4. Connectivity metrics may be distorted

Although ideal Beer–Lambert assumptions would suggest a strict correlation (such that imaging of shading variation could be directly interpreted as density variation), modern scanners do not accurately follow these laws due to scatter and polychromaticity, adding further complexity to the interpretation of grey-values and demonstrating the necessity for physically grounded segmentation approaches [35].

For this reason, the quality of segmentation is fundamental for the accuracy and thus, reliability, reproducibility, and comparability of descriptors between samples.

1.4.5. Segmentation Approaches Used in Previous Research

Existing studies using X-ray computed tomography to study filler dispersion in polymer composites typically use grey-value threshold segmentation to differentiate between filler phases and the surrounding polymer matrix. Ferreira et al. showed that the use of consistent threshold parameters across all analysed samples guarantees that differences in measured particle characteristics correspond to true disparity in filler dispersion, instead of segmentation artefacts [37].

CT segmentation has also been applied to separate filler particles in heterogeneous polymer systems through attenuation contrast between the fillers and the matrix. The reconstructed volumes after phase separation can be directly used to extract quantitative descriptors (for example, particle size distribution and characteristics of the particle population) that help assess the quality of filler dispersion in the composite material [38].

Alongside morphometric descriptors, few studies have employed structural or network-based approaches to measure the spatial organisation and connectivity of fillers in composite materials. Such analyses allow the relation between the material's internal microstructure and mechanical behaviour, as filler distribution and connectivity affect load transfer and damage propagation in composites [39].

1.4.6. CT Analysis-Derived Quantitative Dispersion Parameters

Descriptors derived from CT data can be naturally categorised into five physically meaningful areas:

- Cluster size statistics
- Measures of interfacial accessibility
- Indicators of spatial homogeneity
- Descriptors of agglomerate compactness
- Network topology characteristics

Cluster and Agglomerate Volumetric Distribution

One of the major geometric indicators of the dispersion quality is the distribution of cluster sizes. Ferreira et al. and Liu et al. characterised this cue using high-resolution three-dimensional particle-size estimates derived from segmented CT datasets of cellulose-reinforced LDPE composites. The results showed that an increase in filler content was accompanied by an increase in the mean particle size; also, it can be seen that agglomeration effects were accentuated [37, 39].

But these changes should not be seen as a straightforward enlargement of particles. Rather, they suggest structural evolution within the composite, in particular a greater likelihood of fibre–fibre interaction and clustering. For concentrations greater than 2 wt% of the filler material, the probability of contact with fibres drastically increases and thus favours aggregation and formation of a more intertwined network [37, 39].

Penumadu et al. quantified three-dimensional volumetric particle size distributions and tracked the number of particles above a certain volume threshold (e.g., > 0.001 mm³) as a measure of bad dispersion. Telloari and Latz treated the large-particle tail of the size distribution as a descriptor of the material's structural defects. Hence, this statistical analysis of volumetric cluster sizes provides a measure of structural heterogeneity and defect severity [38].

In contrast to the surrounding matrix, this increase in cluster size, as measured by CT, reflects larger stiffening regions. They also disrupt the continuity of stress, thereby causing high tensile stresses in local regions. Consequently, large agglomerates hinder load sharing and favour premature interfacial failure or crack nucleation. On the contrary, an endowment in which smaller clusters prevail and multipolar mediations are less endowed provides structural conformity, with a decreased risk of failure from critical defects [38].

Filler Surface Area (Interfacial Accessibility)

Beyond size, Ferreira et al. integrated slice-wise measurements across the reconstructed stack to compute total fibre surface area within a defined 3D volume of interest. Especially in the modified-cellulose system, a higher measured surface area at 20 wt% was taken as evidence for better dispersion and less aggregation. Critically, here surface area serves as a structural proxy for matrix–filler interfacial accessibility. Whilst total filler volume may be constant, agglomeration of the fibres leads to loss of accessible surface area, as contact between the fillers occurs. The CT-derived surface area reflects the effective reinforcement interface, rather than just filler content. Thus, from a mechanical point of view, the largest observed surface area from CT analysis implies that extensive matrix–filler contact emerges. This extended interfacial area enhances interfacial shear-transfer for a better stiffness development of the composite. When agglomeration happens, on the other hand, filler–filler contacts reduce the surface area open for matrix accessibility and thereby decrease effective reinforcement area. This leads to a lower efficiency of stress transfer, although the total filler content is unaffected. Thus, surface area should be viewed here not so much as a measure of impurities/nonspecific fillers but rather in terms of how effective you are at reinforcements [37].

Spatial Homogeneity (Local Concentration Fluctuation)

Li et al. studied and characterised dispersion and homogeneity by reconstructing the 3D volume into smaller sub-regions and calculating, for each sub-region, the local standard deviation (STDEV) of fillers based on their volume fraction (ϕf). A higher STDEV indicates a different level of filler concentration, with the filler scattered throughout [39].

This parameter indicates not the degree of size of agglomerates, but the uniformity of filler distribution in different parts of the same sample. Or a material may be composed of relatively small clusters, but still display major differences in the concentration of fillers across spatial regions. The use of STDEV enabled the authors to assess the spatial uniformity of the filler distribution independently of geometric metrics such as cluster size [39].

This gives the metric a notion of spreading ahead of cluster size or compactness, since it represents how evenly distributed the reinforcement is in this analysed volume [39].

Agglomerate Compactness & Specific Surface Area

Li et al. developed a model of 3D multiscale dispersion to reveal how interactions between the filler and the polymer matrix dominate the internal organisation of agglomerates and the resulting connectivity of filler networks. Doubling the SSA was linked with lesser compactness, consistent with a more open agglomerate morphology. This parameter distinguishes dense and compact clusters from branched and open agglomerates. Two aggregates with comparable volume can vary considerably in compaction, and this structural difference influences both the potential for interfacial

interaction and the network-forming ability. Thus, SSA adds to cluster-size analysis by incorporating internal structural organisation [39].

In other words, lower stiffness variations in the filler content hint towards better stress distribution of mechanical loading. However, uniform distribution alone does not guarantee better mechanical properties, as the overall response — particularly in dynamic or high-strain domains — can still be dominated by network connectivity and agglomerate structure. Thus, homogeneity cannot be analysed in isolation; it should be assessed alongside the topology-related descriptors underlying the network architecture and structural interactions [39].

Well-isolated, stiff inclusions of tightly agglomerated, sparsely strewn blobs weakly couple to the surrounding matrix, thereby creating considerable stress concentration in their vicinity. On the contrary, weakly ranging agglomerates and a broader specific surface area (SSA) improve interphase availability, allowing redistribution of stress and establishing a continuous filler network. Therefore, the compactness of clusters provides information on whether they act as local stress raisers, with limited structural activity and a limited effect on the continuity and load-sharing potential of the network [39].

Network Topology: Branching Degree and Connectivity

Most advanced structural descriptors were network topology measurements shown via skeletonisation of CT volumes. Quantified connectivity and branching at agglomerate-scale branch models (e.g., NBN-B/NTN-B, NS-B, LS-B, NBranch) based on 3D-STEM and micron-scale network metrics (e.g., NBN-N/NTN-N, NS-N, LS-N, NNetwork) based on CT skeletons [38, 39].

Significantly, they demonstrated that agglomerate structure at the nanoscale determines network topology at the micron scale such that linear relationships exist between agglomerate-scale and network-scale parameters (e.g., LS-B vs LS-N) [39]. The multiscale coupling shows that the dispersion descriptors do not function independently, and the morphology of agglomerates dictates how the network connectivity builds up. Connectivity metrics determine whether the fillers are homogeneously distributed or are distributed across an integrated load-bearing network. Branching degree describes network density with a cross-bridge. This makes for a set of descriptors that elevate dispersion from the geometric realm into the topological [38].

These extracted descriptors do not correspond to the same structural feature, but each captures a different mode of spatial dispersion within the material:

- Cluster size → Heterogeneity characteristic scale
- Surface area → degree of effective matrix–filler interfacial availability
- STDEV of ϕf → degree of spatial uniformity in filler distribution
- SSA specific surface area → degree of internal compaction within agglomerates
- Connectivity/branching metrics → architecture and filler network topo continuity

These parameters, together, result in complementary perspectives—describing dispersion from geometric, statistical, and topological points of view rather than as a single unified characteristic.

As the network connectivity further evolves, filler particles cease to be dispersed as single islands and instead become interconnected into a percolated load-bearing skeleton. This overlap also provides mechanical stresses with redundant paths through the assembly, further increasing stiffness and

enhancing the composite response in a broad sense. Upon cyclic loading or high degrees of deformation, part of the network can be restructured, or junctions can be lost. Such structural changes give rise to nonlinear viscoelastic behaviour and potential progressive softening in dynamic or large-strain regimes. As a result, it is connectivity that ultimately dictates if the dispersed phase provides static strengthening of the material or, instead, some strain-sensitive dynamic mechanical response [35, 37, 39].

Combined, these features provide the mechanical foundation for experiencing dispersion beyond traditional visual inspection. They relate dispersion directly to stress transfer efficiency, defect site density and severity, as well as the load carried by an internal filler network. In a nutshell, the mechanics under such conditions are dictated not only by filler volume fraction per se but rather by the sparsely connected structural topography and heterogeneity of a system, which can be extracted quantitatively as CT-based parameters.

1.5. Research Gaps and Proposed Approach of the Present Study

The internal microstructure of polymer composites, specifically the filler distribution inside their polymer matrix, strongly influences the mechanical performance of these materials. How these stresses are transferred across the material, affecting its structural integrity and carbon footprint, is a factor of filler dispersion, particle agglomeration, porosity, and inclusions. As highlighted in previous sections, a large body of work has demonstrated that fillers can enhance the mechanical properties of polymer composites significantly as long as they are dispersed homogeneously within the matrix.

It is still difficult to accurately describe the internal microstructure of polymer composites. Researchers usually study filler distribution and composite structure utilising methods such as (SEM) scanning electron microscopy (SEM) and optical microscopy. These methods provide detailed images, but they show only two-dimensional slices of the sample and cover only limited areas. However, polymer composites have three-dimensional internal structures. As a result, 2D images cannot fully show how fillers are spread throughout the material. Also, internal defects such as agglomerates, pores, and inclusions may not appear in the selected slices and can go unnoticed. Because of this, conclusions drawn from these limited views may not reflect the composite's true microstructure, leading to unreliable measurements of filler distribution and its internal defects.

Turning to the solution of this problem, the three-dimensional (3D) characterisation techniques have thus gained significant importance recently to overcome these limitations. X-ray computed tomography (CT) is one such widely used non-destructive technique able to investigate the internal contents of materials. It allows us to clearly observe the whole volume and internal structure of the used sample and to see almost everything inside it quantitatively to evaluate it. CT enables 3D reconstruction of the internal microstructure without sectioning a sample, revealing fillers included for conduction or other purposes, as well as defects and structural heterogeneities distributed over an entire volume of material.

This study applies internal visualisation of polymer composite samples by X-ray CT with further analysis and 3D rendering of the reconstructed datasets in VGStudio MAX. Significant structural features, including porosity, inclusions, filler location, and agglomeration, are identified and quantified in the CT volumes. The study intends to use segmentation and quantitative analysis in order to derive crucial insights regarding the composite's microstructure. This strategy enables a high-

resolution three-dimensional assessment of structural heterogeneity and subsequently improves the insight regarding filler distribution and internal defects in polymer composites.

2. Materials and Methods

2.1. Samples

Six composite samples were investigated in order to study the internal microstructure and porosity characteristics of piezocomposite materials. The studied materials include *barium titanate (BTO) piezocomposites* containing pores and reduced *graphene oxide (rGO) piezocomposites* with various graphene contents, with three samples for each material system.

They were prepared by an extrusion process. To study the influence of processing on the internal structure of the composites, up to three extrusion passes were performed. The processing conditions, influence on differences in filler dispersion and internal porosity in the polymer matrix were investigated. Each sample received a unique code name. Their main features, such as material type and size, are listed in Table 1, and also Fig. 12 shows representative images of the samples, highlighting the look and shape of both BTO and rGO piezocomposites.

Table 1. Overview of investigated samples, including material type, code name, and number of extrusion passes.

Sample Code	Material Type	Number of extrusion passes
BT080_F1	BTO piezocomposite	1
BT080_F2	BTO piezocomposite	2
BT080_F3	BTO piezocomposite	3
rGO8_F1	rGO piezocomposite	1
rGO8_F2	rGO piezocomposite	2
rGO8_F3	rGO piezocomposite	3

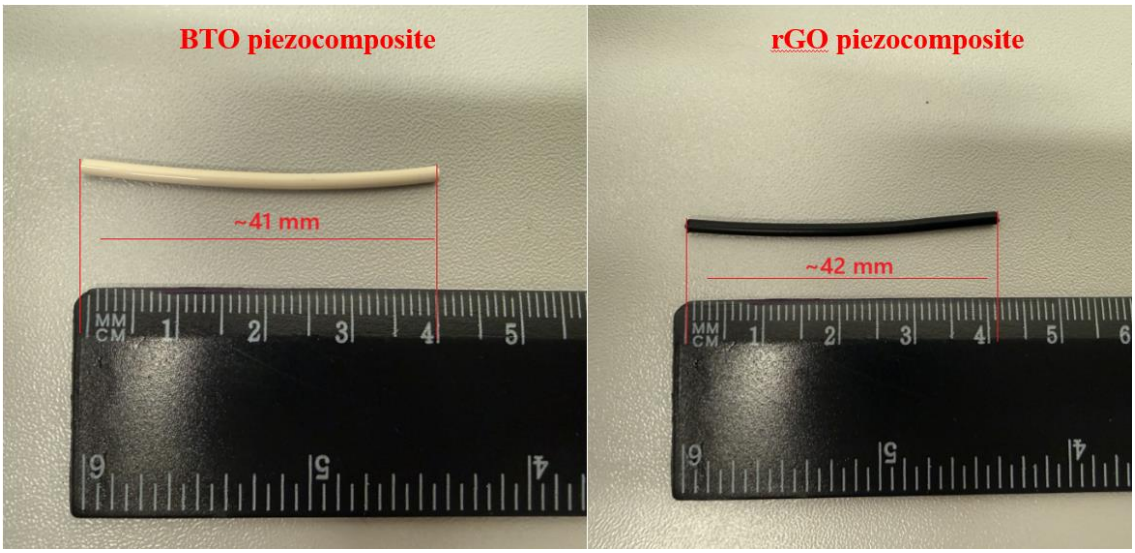

Fig. 12. Representative images of the investigated piezocomposite samples: (a) BTO piezocomposites and (b) rGO piezocomposites

2.2. X-ray Computed Tomography Inspection Parameters

The internal structure of the samples was investigated using X-ray computed tomography (CT), which provides non-destructive three-dimensional imaging of the internal microstructure of materials. It allows the detection and quantitative evaluation of internal defects such as pores, voids, and structural inhomogeneities without destroying the samples.

The principle of X-ray computed tomography (CT) is depicted schematically in Fig. 13 As illustrated in the figure, we mount the sample on a rotating stage and illuminate it with an X-ray beam. The detector takes multiple projection images at different angles when rotating. These projections are then processed and reconstructed by computational algorithms to give a three-dimensional representation of the internal structure of the sample [40].

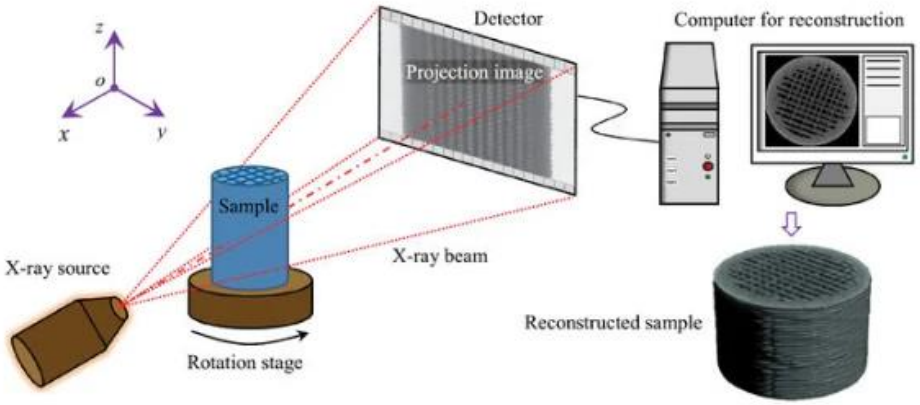

Fig. 13. Schematic representation of the X-ray computed tomography (CT) principle

Fig. 14 also displays images of the CT system utilised in this investigation at KTU Ultrasound Research Institute. Measurements were conducted using a RayScan 250E, a three-dimensional X-ray computed tomograph equipped with a 225 kV micro-focus X-ray source.

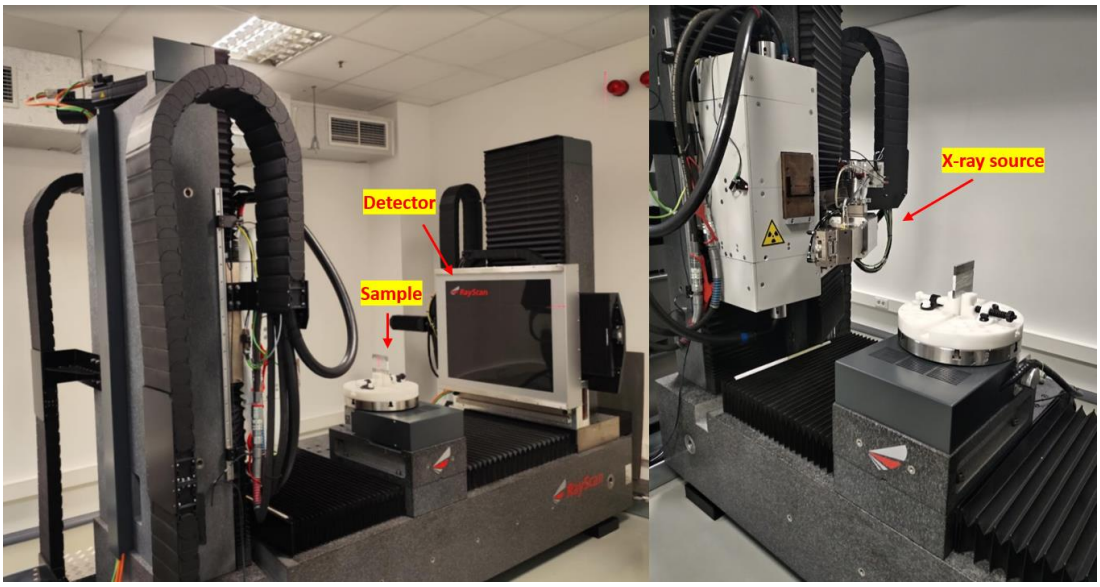

Fig. 14. RayScan 250E CT system used for experimental investigation

CT scanning was performed using parameters shown below:

- Voltage: 160 kV
- Current: 80 µA
- Integration time: 2000 ms
- Number of projections: 1800
- Voxel size: 7 µm

These scanning conditions allow for sufficient resolution to accurately detect internal defects, such as pores, inclusions, etc., within the analysed composite samples.

2.3. Image Processing and Porosity Analysis Procedure Workflow

The General workflow, starting with the main stages of work and image processing for porosity analysis of this work, is presented in Fig. 15 and Fig. 16 The CT image data was processed in VGStudio MAX, performed through a series of process steps, such as data import, region selection, surface determination, porosity analysis, and export of quantitative results.

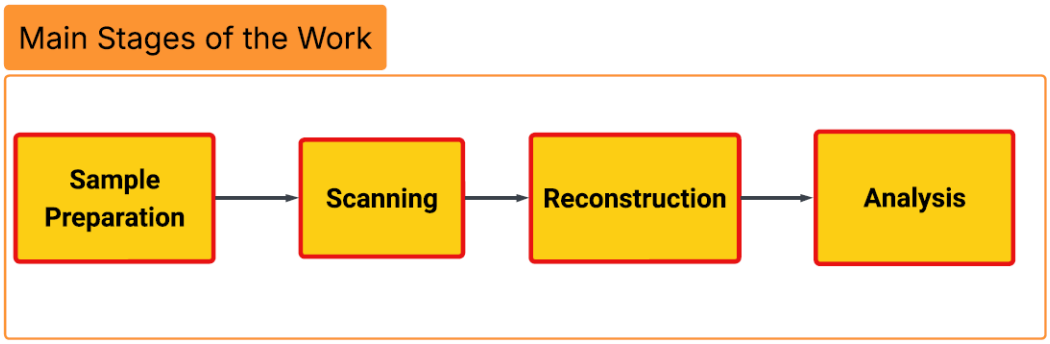

Fig. 15. Main Stages of Investigation

The investigation started with sample preparation, as samples were scanned using X-ray CT after being prepared. The projection data obtained from the acquired scans were reconstructed to obtain 3D datasets of the samples. Next, these reconstructed datasets were used for subsequent image processing and quantitative analysis. The order of these stages reflects the setup of this study. It also demonstrates that the investigation was conducted in an adequately systematic and logically sequenced manner.

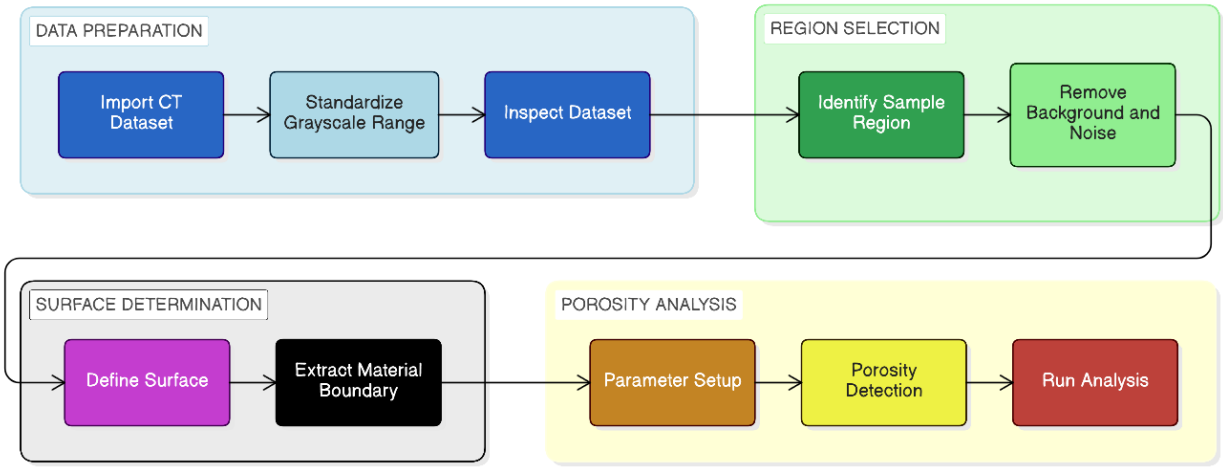

Fig. 16. Workflow of image processing and porosity analysis in VGStudio MAX, including data import, region selection, surface determination, porosity analysis, and export of quantitative results

The reconstructed CT datasets were imported with the same grayscale scale to normalise and to make sample comparison feasible. Datasets were previewed and inspected post-import, prior to any further processing.

Import settings used for all samples :

- default range (0 to 65535)
- selected range for sample (Lowest gray value :0, Highest gray value: 65535)

The next step was to define the sample area and exclude unwanted regions of background by selecting the relevant analysis region. Once the region was selected, surface determination was performed for the given volume. The volume was selected from the Scene Tree, and separate functions were applied to determine the Surface type based on similar settings for each of the sampled data. Using these parameters, the material surface from the grayscale distribution of the dataset was produced. Threshold value used for the surface determination was 2145 units and threshold for inclusion was 7200 units.

Surface determination parameters used for the BTO piezocomposite samples :

- Search distance: 3.000 voxel
- Filter voids: Remove small voids

The search distance was changed to 3.000 voxels to determine the material boundary in the surface determination step, and the Remove small voids option was turned on to remove very small void-like features that are likely a result of noise. After having applied these settings, the material surface was generated according to the dataset grayscale distribution. After determining the surface, next came the analysis in their software Porosity/Inclusion area. The pore detection used was VGEasyPore.The pore detection used was VGEasyPore. VGEasyPore determines pore boundaries by using a local grayscale histogram to calculate a local threshold for each analysed pore region. This allows the pore to be separated from the surrounding material based on local grayscale differences. The method also provides subvoxel accuracy by adjusting the pore boundary according to the grayscale values of neighbouring voxels. In this way, VGEasyPore enables quantitative evaluation of pore characteristics such as diameter and shape-related parameters. Thus, internal holes can be detected and statistically characterised depending on their distribution, size and shape. This technique analyses greyscale discrepancies between the solid material and air-filled voids in the reconstructed CT dataset to

identify pores as low-density empty areas inside the material. Internal holes may thus be found and statistically assessed based on their distribution, size, and form [41].

The parameters used for VGEasyPore/porosity analyses are shown below:

- Contrast: 20 %
- Local area size: 10 vox
- Surface distance: 1 voxel

The reliability of pore identification was directly influenced by several parameters, particularly contrast, local area size, and surface distance. The contrast parameter was important because it controlled how distinct a pore had to be from the surrounding material in order to be identified. If the contrast was too low, noise or weak artefacts could be detected as pores, whereas if it was too high, smaller or less distinct pores could be missed. The local area size parameter influenced the evaluation of the surrounding region during pore detection and therefore contributed to the stability of the analysis. In addition, the surface distance setting helped reduce false detections near the specimen boundary, where grayscale transitions and reconstruction effects are more likely to produce non-physical indications. Thus, these parameters were important for achieving sensitive and stable pore detection in the analysed datasets.

Exported Quantitative Parameters From Porosity Analysis

The analysis parameters were exported from the software as an Excel file for further analysis. The exported dataset contains multiple parameters, such as (e.g., pore diameter, sphericity, radius, voxel position, projected sizes, and projected areas).

The parameters used for the quantitative analysis carried out in this analysis are as follows:

- Diameter [µm]
- Sphericity

These parameters were used to analyse the pore size distribution, the shape characteristics of detected pores, and the sphericity distribution.

2.4. Inclusion Analysis Procedure

Turning to analyse inclusions, rGO piezocomposite samples were imported in the same way using the same procedure as before. The same surface determination settings were used again to keep all datasets consistent. After the surfaces were defined, the inclusion analysis was performed in the Porosity/Inclusion section of VGStudio MAX. The VGDefX/Only threshold method was used to detect inclusions. In this approach, the inclusion detection was based on thresholding of grayscale values in the reconstructed CT volume. The VGDefX algorithm uses the material gray value from the histogram as a reference and allows the threshold to be adjusted relative to the mean gray value. It can also use the determined surface as a starting contour or as a filter for potential defect candidates. The Only Threshold method, in contrast, just performs thresholding without any additional algorithm-based filtering, and it makes sense to compare directly the detected indications with the result based on VGDefX. Therefore, the combined use of VGDefX/Only Threshold helped to identify high-density inclusion-like regions and extract their quantitative characteristics from the CT data [42].

The chosen algorithm for the inclusion analysis was VGDefX. Accompanied by a manually defined material definition, the indication type was assigned as Inclusion. The lowest gray value of inclusion

was limited to 7200. Also, result filtering was undertaken to ensure data quality. As an initial step, indications for which the voxel dimension reflected less than eight voxels on any axis were excluded as being artefacts. We also enabled the Ignore streak artifacts option to minimise the impact of CT artefacts, which results in more accurate outcomes.

After inclusion analysis, a lot of parameters were exported from VGStudio MAX. These encompassed various geometrical and spatial features observed in inclusions.

This study focused on two main parameters:

- Diameter [µm]
- Volume [µm^3]

The diameter parameter shows the equivalent size of the detected inclusions and was used to evaluate how their sizes are distributed. The volume parameter gives a better measure of inclusion size in three dimensions. Larger volume values mean there are clusters or groups of inclusions, while smaller values show the particles are more spread out. Because of this, volume was used to study how inclusions group together and how different the structure is within the samples.

3. Results and Discussion

This chapter describes and discusses the findings resulting from the X-ray computed tomography of the investigated polymer composite specimens. Both qualitative visual inspection of the internal structure and quantitative characterisation of the internal defects were performed on the reconstructed CT data sets. Slice images and 3D reconstructions were analysed to determine the most prominent defects in each type of material system. Subsequently, quantitative characterisation of pore-related defects in BTO and inclusion-related defects in rGO was carried out.

3.1. Visualisation of Internal Structure and Defect Features

Prior to the presentation of the quantitative analysis, the CT reconstructions were visually inspected so as to allow for the comparison of internal structures of the studied samples and identification of the primary defects occurring in the respective materials. This was achieved by using representative slices and 3D visualisation to provide an overall impression of internal morphology of the sample.

The top-view cross-sections of the BTO piezocomposite materials are depicted in Fig. 17 The cross-sectional slices allow for the visualisation of the inner structures of the samples, and the comparison of the observable defects in an easy-to-make way. It can be seen from the illustrations that the BTO samples have different inner structures and defects. This was the initial visual analysis before any numerical evaluation. Through the examination of the CT slices, it can be observed that the presence of pore-type defects constitutes the most common internal characteristic within the BTO material system. Porosity analysis would then be performed on the BTO specimens below. Apart from that Top-view cross-sectional comparison of the rGO piezocomposite samples are shown in Fig. 18.

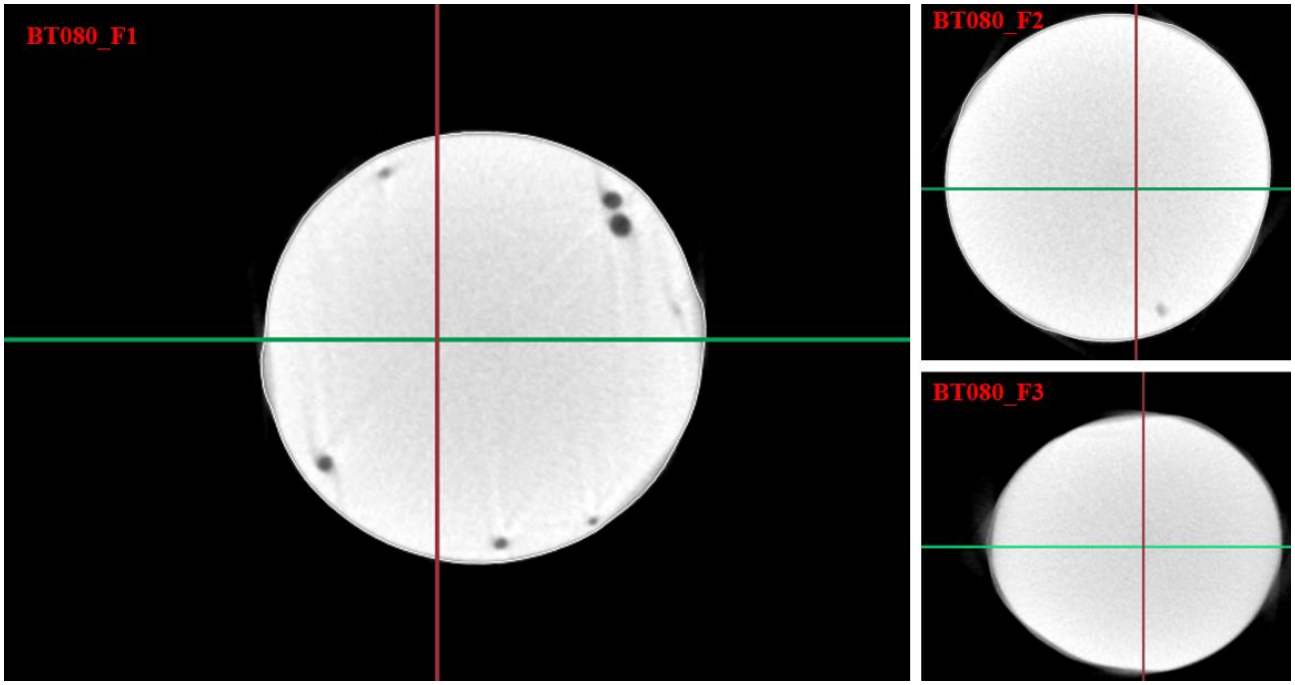

Fig. 17. Top-view cross-sectional comparison of the BTO piezocomposite samples

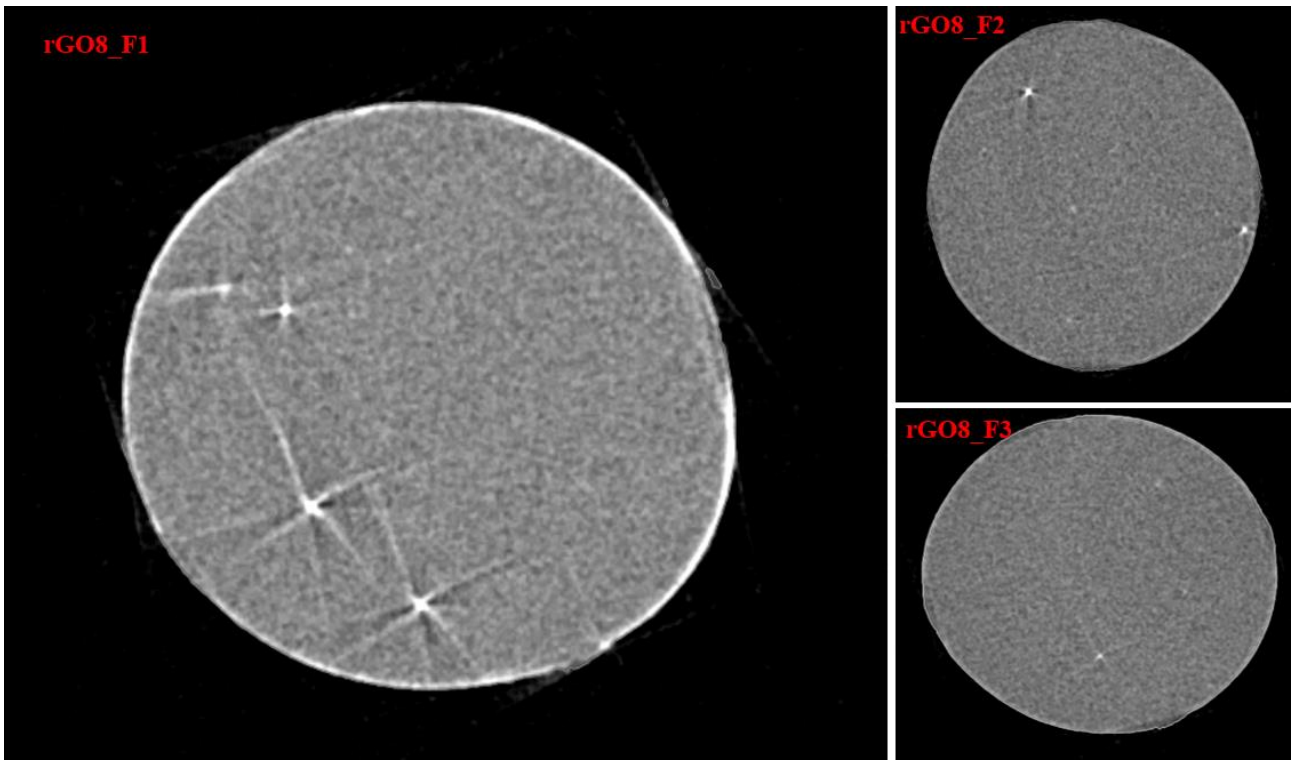

Fig. 18. Top-view cross-sectional comparison of the rGO piezocomposite samples

3.2. Pore Diameter Distribution

The pore diameter measurements were obtained from the porosity analysis, which was performed using the VGEasyPore method. This is a quantitative analysis of the pore size distribution on BTO piezocomposite samples. The results obtained show a clear difference between the samples. Sample-BT080_F1 has a large number of pores spanning a wide range of diameters. The largest number of medium-sized pores is observed in the 50–100 µm and 100–200 µm ranges. In contrast, Sample-BT080_F2 has many fewer pores than the sample-BT080_F1 mentioned above. The size of the majority of pores lies between 0–10 µm and 10–25 µm, while only a few pores exist in larger size ranges. Among the samples, Sample-BT080_F3 has the least number of pores, and these are only in the smallest diameter ranges. This pattern suggests a denser and more structurally homogeneous material since it shows that the number of pores decreased along with a shift toward smaller defect sizes. In larger intervals, they are not observed, which suggests a higher density of the internal structure. The lack of bigger pores is particularly crucial from the standpoint of material performance because these flaws are more likely to serve as sites of stress concentration and lower structural reliability. Because there is a noticeable improvement in internal homogeneity from BT080_F1 to BT080_F3, the difference between the samples is significant both quantitatively and structurally. Table 2 presents the pore diameter distribution across all samples and summarises the differences between the diameter ranges. For better understanding, the same data is represented graphically in Fig. 20 Three-dimensional reconstruction images of the sample are shown in Fig. 19 The distribution of pores was also concordant with quantitative analysis. Sample-BT080_F1 has the highest number of pores as compared to Sample-BT080_F2 and Sample-BT080_F3, showing a dense structure with less porosity

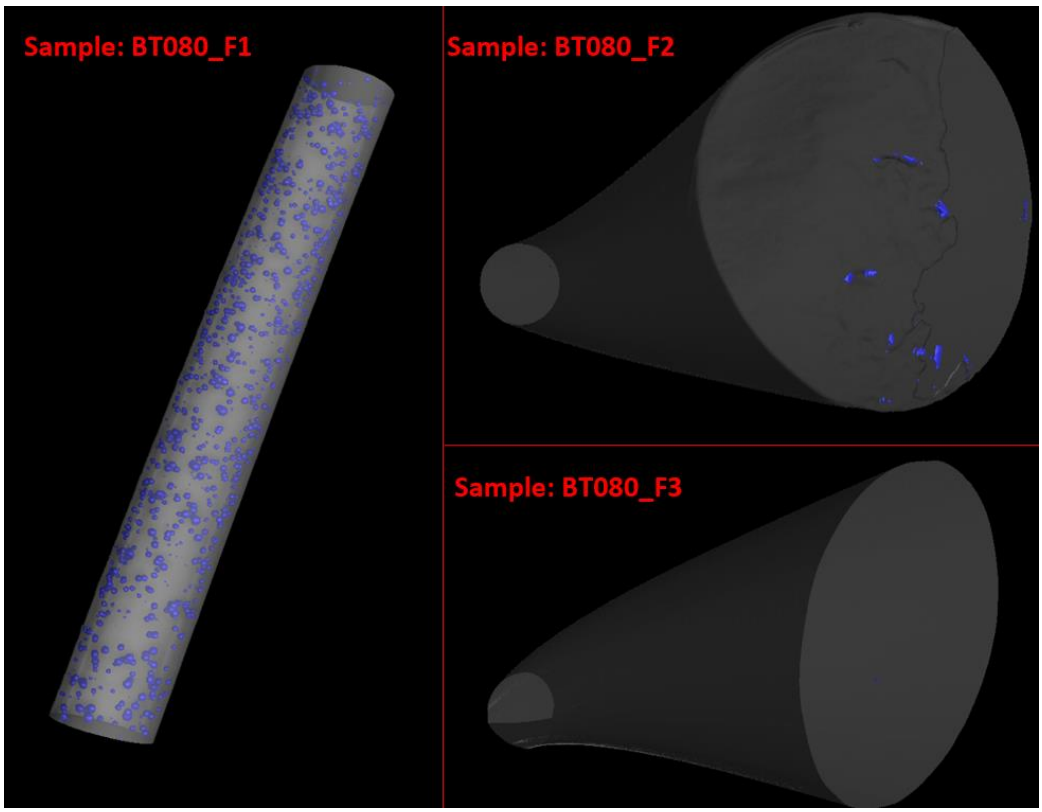

Fig. 19. Three-Dimensional Visualisation and Porosity Analysis of Samples

Table 2. Pore diameter distribution of all samples based on VGEasyPore analysis

Diameter Range (µm)	Number of Pores Sample-BT080_F1	Number of Pores Sample-BT080_F2	Number of Pores Sample-BT080_F3
0–10	30	35	4
10–25	74	19	3
25–50	138	8	1
50–100	267	7	0
100–200	407	5	0
200–300	48	0	0
300–400	15	0	0
>400	1	0	0

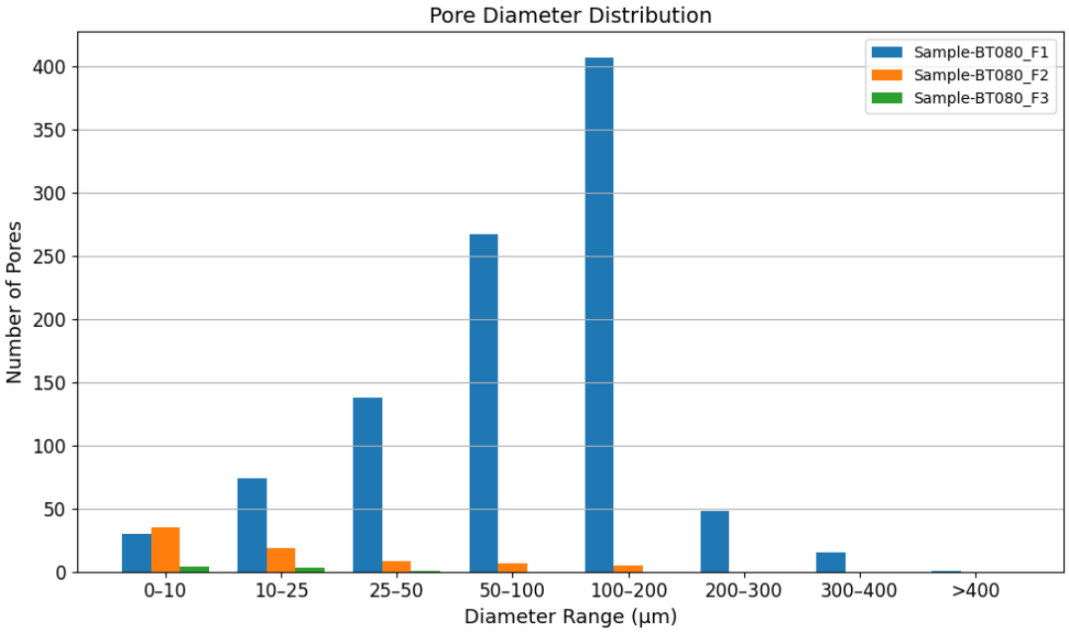

Fig. 20. Pore diameter distribution of all samples across different size ranges

Three-dimensional reconstruction images of the sample are shown in Fig. 19 The distribution of pores was also concordant with quantitative analysis. Sample-BT080_F1 has the highest number of pores as compared to Sample-BT080_F2 and Sample-BT080_F3, showing a dense structure with less porosity.

3.2.1. Pore Sphericity Distribution

Porosity analysis was also used to calculate sphericity values. This is a nondimensional parameter that varies between 0 and 1, with values close to 1 indicating more spherical pores. The results vary widely from sample to sample. For Sample-BT080_F1, highly spherical pores dominate the pore size distribution, and most of these fall in the range 0.8-1.0. This means that the shape of most pores is regular and well defined. This is significant because pore shape helps differentiate between more irregular defect morphology and more regular voids by offering information beyond pore count alone.

Conversely, Sample-BT080_F2 has a wider range of distribution, which mainly ranges from 0.2 to −0.6. This indicates that there are more non-uniform pores. The wider distribution in Sample-BT080_F2, on the other hand, indicates a more varied internal structure due to the higher variety in pore shape. Turning to Sample-BT080_F3, which has the fewest pores, most of which are focused in the range of 0.4–0.8; though quite limited porosity can be observed, mostly with moderately regular shapes. The sphericity distribution for all samples is presented in Table 3, while the graphical representation is shown in Fig. 21.

Table 3. Pore sphericity distribution of all samples based on VGEasyPore analysis

Sphericity Range	Sample-BT080_F1	Sample-BT080_F2	Sample-BT080_F3
0–0.2	6	10	0
0.2–0.4	27	33	0
0.4–0.6	14	29	6
0.6–0.8	76	2	2
0.8–1.0	857	0	0

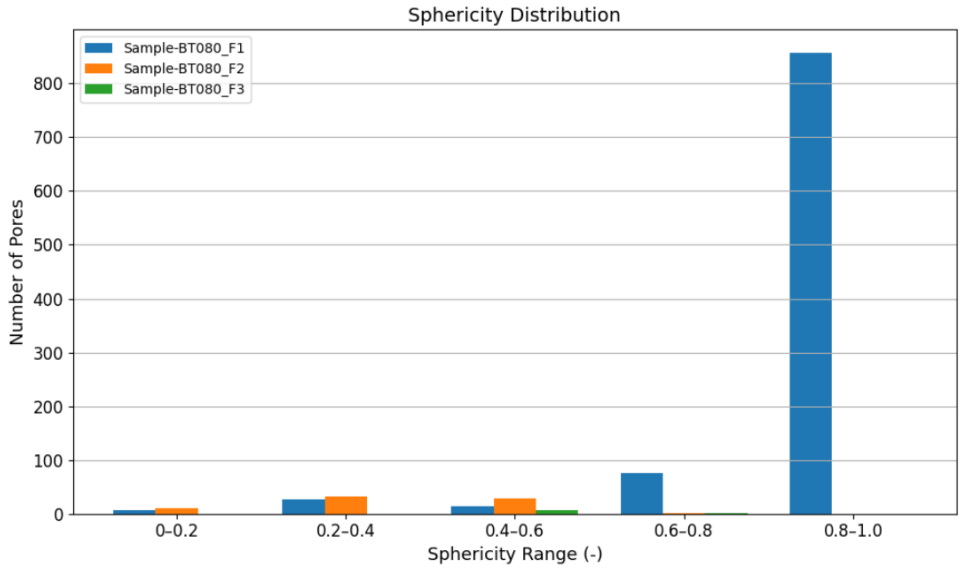

Fig. 21. Pore sphericity distribution of all samples across different ranges

Overall, the porosity analysis shows a significant difference between samples, both for pore size and sphericity. Sample-BT080_F1 shows more porosity with bigger and rounder pores. In comparison, Sample-BT080_F2 features smaller pores of lower sphericity, and Sample-BT080_F3 has a more closely packed structure with less porosity. These results demonstrate that processing conditions directly determine pore formation, size distribution, and sphericity of the pore structure, eventually controlling the structural uniformity of the material. Because sphericity revealed both the number of pores and how their geometrical characteristics varied between samples, it was a helpful supplemental measure.

3.3. Inclusion Diameter Distribution

The VGDefX/Only threshold technique was applied to find the inclusion diameters. It can be seen that there are visible distinctions between the rGO piezocomposites. For all three samples, most of the inclusions are found in the sizes of 25-50 µm and 50-100 µm. Inclusion structures have a significantly larger amount in Sample-rGO8_F1, most of which fall into the range of 25-50 µm. It means that this size range is the most characteristic for comparing the difference of inclusion structures in the samples under analysis. As for the inclusions in Sample-rGO8_F2 and Sample-

rGO8_F3, their quantity is significantly lower. Despite the similarity in distribution, the presence of inclusions is less intensive here. Inclusions exceeding 100 µm can be rarely seen in any of the samples considered. All inclusion diameter distributions can be found in Table 4, whereas Fig. 22 illustrates this information graphically.

Table 4. Inclusion diameter distribution of all samples across diameter ranges [µm] based on VGDefX/Only threshold analysis

Diameter Range (µm)	Number of Inclusions Sample-rGO8_F1	Number of Inclusions Sample-rGO8_F2	Number of Inclusions Sample-rGO8_F3
0-10	0`	0	0
10--25	128	28	43
25-50	1061	197	176
50-100	519	76	77
100-200	106	11	8
200-300	3	1	3
300-400	1	0	0
>400	1	1	0

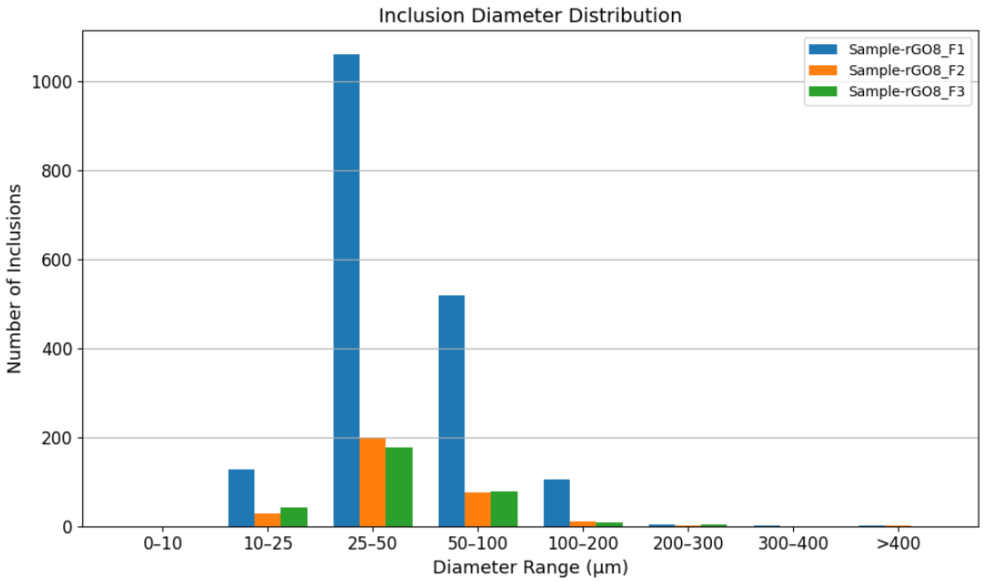

Fig. 22. Inclusion diameter distribution of all samples across different size ranges [µm]

Inclusion Volume Distribution

The inclusion volume was calculated with the aid of the VGDefX/Only Threshold Analysis. Volume data is relevant in this analysis since it provides a three-dimensional approach when determining inclusion severity, instead of relying on diameter data only. There is evident distinction between the inclusion volume results for the rGO piezocomposites. Most inclusions in all samples are found in

the ranges of 5,000-10,000 µm³ and 10,000-50,000 µm³. Sample-rGO8_F1 contains many inclusions in the above ranges, indicating high agglomeration. On the other hand, Sample-rGO8_F2 and Sample-rGO8_F3 have few inclusions. Although their distribution is similar, the intensity in terms of number of inclusions is low. Very few inclusions are observed for volumes above 100,000 µm³. The full inclusion volume distribution is given in Table 5 and graphically presented in Fig. 23.

Table 5. Inclusion volume distribution of all samples across volume ranges [µm³]

Volume Range (µm³)	Number of Inclusions Sample-rGO8_F1	Number of Inclusions Sample-rGO8_F2	Number of Inclusions Sample-rGO8_F3
0–1,000	0	0	0
1,000–5,000	547	62	58
5,000–10,000	548	76	63
10,000–50,000	616	133	116
50,000–100,000	68	27	24
100,000–300,000	36	13	8
300,000–600,000	2	2	1
>600,000	1	1	2

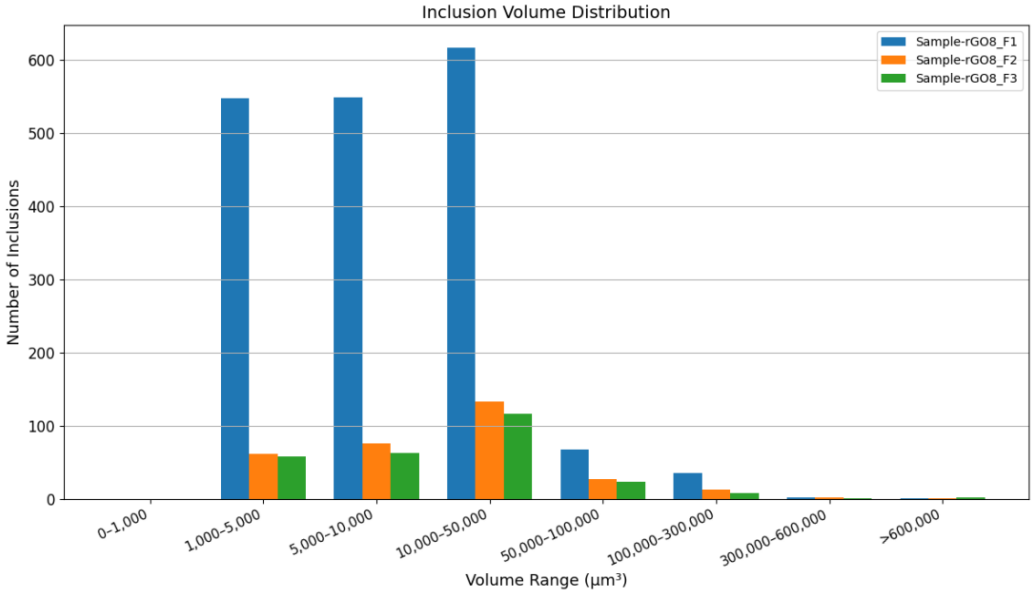

Fig. 23. Inclusion volume distribution of all samples across different ranges [µm³]

The results show that both the number and size of inclusions decrease from Sample-rGO8_F1 to Sample-rGO8_F3. Most inclusions are found within a narrow range of diameters and volumes. This pattern can also be seen in the 3D comparison in Fig. 24, where Sample-rGO8_F1 looks more varied, while Sample-rGO8_F2 and Sample-rGO8_F3 have a more compact and uniform structure.

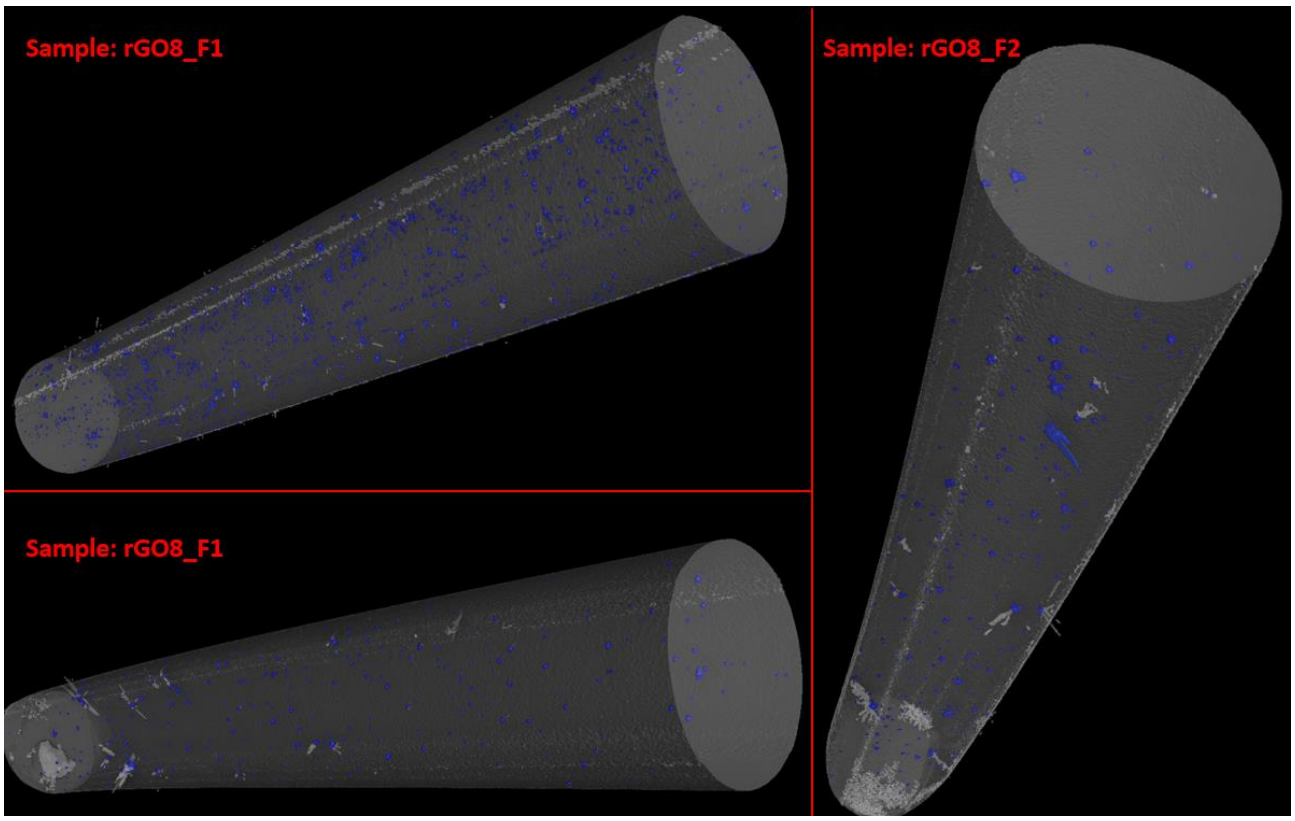

Fig. 24. Three-dimensional comparative view of all samples showing inclusion distribution and structural differences

Overall, it can be concluded that the detected distinctions between the specimens under consideration mainly concern the amount of flaws and their presence within the specimen. The flaw content is maximum in the first condition specimens; however, in the case of the latter condition specimens, there is a distinct reduction in the number of flaws inside the specimen. Thus, it can be presumed that the change in the condition leads to better structural homogeneity. Furthermore, the reduction in the amount of pores and inclusions indicates a denser internal structure.

Conclusions

1. The analysis of earlier studies showed that X-ray computed tomography is better suited than traditional 2D techniques for assessing filler dispersion in polymer composites because it offers complete 3D visualisation of the sample and allows quantitative evaluation of pores, inclusions, agglomerates, and structural heterogeneity. The findings also suggest that uneven dispersion and agglomeration cause stress concentration, lower load transfer efficiency, and reduce mechanical performance.
2. From the barium titanate (BTO) piezocomposite with 1 extrusion pass to the BTO piezocomposite with 3 extrusion passes, the number of pores dramatically dropped, with the maximum concentration found in the 100–200 μm and 50–100 μm diameter ranges. The most noticeable variation in the reduced graphene oxide (rGO) piezocomposites was found in the 25–50 μm inclusion size range, where the number of inclusions significantly dropped from the sample with 1 extrusion pass to the samples with 2 and 3 extrusion passes. These findings show that as extrusion passes increase, the fault content clearly decreases and structural homogeneity improves.
3. CT-derived structural characteristics were used to evaluate the link between filler dispersion and composite properties. Pore content dropped from the BTO piezocomposite with 1 extrusion pass to the BTO piezocomposite with 3 extrusion passes, and inclusion levels were lower in the rGO piezocomposites with 2 and 3 extrusion passes than in the sample with 1 extrusion pass. The BTO and rGO piezocomposites with 3 extrusion passes showed the most consistent internal structure and the lowest defect content among the examined samples, suggesting the highest dispersion quality as well as better mechanical performance and durability.
4. Dispersion quality was clearly impacted by processing factors. In both material systems, structural flaws decreased as the number of extrusion passes rose from one to three. The total number of pores in the BTO series decreased from 980 in the sample with 1 extrusion pass to 74 in the sample with 2 extrusion passes and 8 in the sample with 3 extrusion passes. The overall number of inclusions by diameter distribution in the rGO series dropped from 1819 in the sample with 1 extrusion pass to 314 in the sample with 2 extrusion passes and 307 in the sample with 3 extrusion passes. The 25–50 μm inclusion range showed the biggest variation, with counts falling from 1061 in the sample with 1 extrusion pass to 197 in the sample with 2 extrusion passes and 176 in the sample with 3 extrusion passes. The inclusion volume data revealed a similar pattern: the number of inclusions in the 10,000–50,000 μm^3 range dropped from 616 in the sample with 1 extrusion pass to 133 in the sample with 2 extrusion passes and 116 in the sample with 3 extrusion passes. These findings indicate that the number of extrusion passes contributes to the homogeneity of structural distribution and lowers agglomeration defects.

List of references

1. KAHAR, Hardinnawirda Binti. Kahar . Online. Bachelor's thesis. Pahang: Universiti Malaysia Pahang, 2012. Available at: https://umpir.ump.edu.my/id/eprint/4908/1/cd7278_84.pdf .
2. KIRAN, M. D., H. K. GOVINDARAJU, T. JAYARAJU та Nithin KUMAR. Review – Effect of Fillers on Mechanical Properties of Polymer Matrix Composites. Materials Today: Proceedings, т. 5 (2018), с. 22421–22424. ISSN 2214-7853. 1
3. VINOD KUMAR, T., M. CHANDRASEKARAN, P. MOHANRAJ, Ravishankar BALASUBRAMANIAN, R. MURALIRAJA and others. *Fillers preparation for polymer composite and its properties – A review* . Online. International Journal of Engineering & Technology, vol. 7 (June 2018), no. 2.33, pp. 212–217. Available at: https://doi.org/10.14419/ijet.v7i2.33.13889 .
4. ROTHON, Roger. *Fillers for Polymer Applications*. Online. Cham: Springer International Publishing, 2017. ISBN 978-3-319-28116-2. Available at: https://doi.org/10.1007/978-3-319-28117-9.
5. WYPYCH, George. *Handbook of Fillers*. 4 in the species. Toronto: ChemTec Publishing, 2016. ISBN 978-1-895198-91-1.
6. CHO, Changwoo, Dongwon KIM, Chaeeun LEE, and Je Hoon OH. Ultrasensitive ionic liquid polymer composites with a convex and wrinkled microstructure and their application as wearable pressure sensors. Online. *ACS Applied Materials & Interfaces*, vol. 15, no. 12, 2023, pp. 13625–13636. ISSN 1944-8244. Available at: https://doi.org/10.1021/acsami.2c22825.
7. KUNDIE, Fathie, Che Husna AZHARI, Andanastuti MUCHTAR, and Zainal Arifin ARIFIN. *Effects of Filler Size on the Mechanical Properties of Polymer-filled Dental Composites: A Review of Recent Developments*. Online. Journal of Physical Science, Vol. 29 (2018), No. 1, pp. 141–165. Available at: https://doi.org/10.21315/jps2018.29.1.10.
8. FU, Shao-Yun, Xi-Qiao FENG, Bernd LAUKE, and Yiu-Wing MAI. Effects of particle size, particle/matrix interface adhesion, and particle loading on mechanical properties of particulate–polymer composites. Online. Composites: Part B, vol. 39 (2008), pp. 933–961. Available at: https://doi.org/10.1016/j.compositesb.2008.01.002.
9. Fracture Toughness of Polypropylene-Based Particulate Composites – PMC. Online. PMC Home. [n.d.]. Available at: https://pmc.ncbi.nlm.nih.gov/articles/PMC5513573/. [Accessed 19.02.2026].
10. JÁNOS MÓCZÓ, tá BÉLA PUKÁNSZKY. Particulate Fillers in Thermoplastics. Online. In: *Polymers and Polymeric Composites: A Reference Series*, pp. 1–43. Berlin, Heidelberg: Springer-Verlag, 2016. Available at: https://doi.org/10.1007/978-3-642-37179-0_7-1.
11. MA, Xinyue, Yasser ZARE, and Kyong Yop RHEE. A Two-Step Methodology to Study the Influence of Aggregation/Agglomeration of Nanoparticles on Young's Modulus of Polymer Nanocomposites. Online. Nanoscale Research Letters, vol. 12 (2017), 621. Available at: https://doi.org/10.1186/s11671-017-2386-0.
12. KUNDIE, Fathie та Che Husna AZHARI. Effects of Filler Size on the Mechanical Properties of Polymer-filled Dental Composites: A Review of Recent Developments. *Journal of Physical Science*, т. 29 (2018).

13. SEGURADO J., GONZÁLEZ C. and LLORCA J. A numerical investigation of the effect of particle grouping on the mechanical properties of composites. *Acta Materialia* , vol. 51 (2003), pp. 2355–2369.
14. RANI, Elizabeth, Murugeswari R, Mariyappan Arul KUMAR, and Siengchin SUCHART. Quantitative assessment of particle dispersion in polymeric composites and its effect on mechanical properties. Online. Journal of Materials Research and Technology, 2022. Available at: https://doi.org/10.1016/j.jmrt.2022.05.147
15. DU, X. M., K. F. ZHENG, та F. G. LIU. Effect of clustering on the mechanical properties of SiCp reinforced aluminum metal matrix composites. *Digest Journal of Nanomaterials and Biostructures*, т. 13 (2018), № 1, с. 253–261.
16. PENG, Xu, Loomis JAMES та Panchapakesan BALAJI. Load Transfer and Mechanical Properties of Chemically Derived Single-Layer Graphene Reinforcements in Polymer Composites. *Nanotechnology*, т. 23 (2012), № 50, 505713. ISSN 0957-4484.
17. *Reinforcement mechanisms in MWCNT-filled polycarbonate* . Online. Stevens Institute of Technology.[n.d.].Access mode: https://researchwith.stevens.edu/en/publications/reinforcement-mechanisms-in-mwcnt-filled-polycarbonate/. [date of access 19.02.2026].
18. VEIGEL, Danielle, Kabir RISHI, and Gregory BEAUCAGE. Comparison of nanocomposite dispersion and distribution for several melt mixers. *Polymer*, vol. 269 (2023). ISSN 0032-3861.
19. GAO, Yi, Zhuo LIN, Allen TANNENBAUM, and Sylvain BOUIX. Automated Dispersion and Orientation Analysis for Carbon Nanotube Reinforced Polymer Composites. *Nanotechnology*, vol. 23 (2012), no. 43, 435706.
20. CHOOBBARI, Mehrdad Lotfi, Jennifer FERGUSON, Niko Van DEN BRANDE, Tim SMITH, and Tatevik CHALYAN. *Studying the concentration of polymers in blended microplastics using 2D and 3D Raman mapping*. Online. Scientific Reports, Vol. 13 (2023), 7771. Available at: https://doi.org/10.1038/s41598-023-35010-0.
21. FENG, Zemin, Jinpan ZHONG, Weijiang GUAN, and Rui TIAN. *Three-dimensional direct visualization of silica dispersion in polymer-based composites*. Online. Analyst, vol. 143 (2018), pp. 2090–2095. Available at: https://doi.org/10.1039/c8an00016f.
22. AIESH, Basel. *Measurement of dispersion barriers through SEM images*. Master's thesis. Uppsala: Uppsala University, 2015.
23. ROTHMAN, Jason Seth, Carolina BORGES-MERJANE, Noemi HOLDERITH, and Peter JONAS. *Validation of a stereological method for estimating particle size and density from 2D projections with high accuracy*. Online. PLOS ONE, vol. 18 (2023), no. 3, e0277148. Available from: https://doi.org/10.1371/journal.pone.0277148.
24. ECHLIN, McLean P., Timothy L. BURNETT, Andrew T. POLONSKY, and Tresa M. POLLOCK. *Serial sectioning in the SEM for three dimensional materials science*. Online. Current Opinion in Solid State & Materials Science, vol. 24 (2020). Available from: https://doi.org/10.1016/j.cossms.2020.100817.
25. ZENG, Charlie, and Stephen J FOSTER. *A stereological approach to estimation of fibre distribution in concrete*. Online. Construction and Building Materials, vol. 324 (2022), 126547. Available from: https://doi.org/10.1016/j.conbuildmat.2022.126547.
26. MOHARANA, Srikanta, Bibhuti B. SAHU, Arpan KUMAR NAYAK, and Santosh K. TIWARI (eds.). *Polymer Composites: Fundamentals and Applications*. Online. Singapore: Springer Nature

Singapore Pte Ltd., 2024. ISBN 978-981-97-2074-3. Available from: https://doi.org/10.1007/978-981-97-2075-0.

27. SINGH, Somya, Hechao LI, Sudhanshu S. SINGH, Jason WILLIAMS, Tyler STANNARD, et al. *Microstructural characterization and mechanical property prediction of a polymer matrix composite by X-ray synchrotron tomography and spatial correlation functions*. Online. SN Applied Sciences, vol. 1 (2019), 1302. Available from: https://doi.org/10.1007/s42452-019-1310-x.
28. LÉONARD, Fabien, Jasmin STEIN, Matthieu GRESIL, and Constantinos SOUTIS. X-ray Computed Tomography for Composites: 3D Non-Destructive Testing. In: *53rd Conference of the British Institute of Non-Destructive Testing*, p. 31. Manchester, United Kingdom, 2014-02-11. [n.d.].
29. AUENHAMMER, Robert Michael. *X-ray computer tomography based numerical modelling of fibre reinforced composites*. Licentiate thesis. Göteborg: Chalmers University of Technology, 2021.
30. GARCEA, S., Y. WANG, and P. WITHERS. *X-ray computed tomography of polymer composites*. Online. Composites Science and Technology, vol. 156 (2018), pp. 305–319. Available from: https://doi.org/10.1016/j.compscitech.2017.10.023.
31. SIETINS, Jennifer M., William H. GREEN, and Justin S. JONES. *Material Evaluation Using X-ray Computed Tomography*. 2018, p. 63.
32. SIETINS, Jennifer M., William H. GREEN, and Justin S. JONES. *Material Evaluation Using X-ray Computed Tomography*. Technical report. Aberdeen Proving Ground, MD: DEVCOM Army Research Laboratory, 2021
33. STRAUMIT, I., I. BARAN, L. FARKAS, C. HAHN, and S. LOMOV. Micro-CT-based analysis of fibre-reinforced composites: Applications. In: *European Conference on Composite Materials (ECCM18)*, pp. 1–8. Athens, Greece, 2018-02-18. [n.d.].
34. SILVA, Henrique V., Nuno P. CATAPIRRA, Marta S. CARVALHO, Telmo G. SANTOS, and Miguel A. MACHADO. *Nondestructive Testing of 3D Printed Fiber-Reinforced Polymeric Composites: An Experimental Critical Comparison*. Online. 3D Printing and Additive Manufacturing, vol. 11 (2024), no. 3, pp. 1196–1208. Available from: https://doi.org/10.1089/3dp.2022.0291.
35. MAIRE, Eric, and Philip J. WITHERS. *Quantitative X-ray tomography*. Online. International Materials Reviews, vol. 59 (2014), no. 1, 0950-6608. Available from: https://doi.org/10.1179/1743280413Y.0000000023.
36. PRIETO, Javier Sánchez, Filippo ZANINI, and Simone CARMIGNATO. New approach to enhance multi-material computed tomography reconstructions by selecting the optimal combination of scanning orientations for multiple scan fusion. Online. In: *NDT & E International*, pp. 256–270. 10290th ed. Amsterdam: Elsevier, 2023. Available from: https://doi.org/10.1016/j.ndteint.2023.102904.
37. FERREIRA, F., G. TRINDADE, L.M.F LONA, J. BERNARDES, and R. GOUVEIA. *LDPE-based composites reinforced with surface modified cellulose fibres: 3D morphological and morphometrical analyses to understand the improved mechanical performance*. Online. European Polymer Journal, vol. 117 (2019), pp. 105–113. ISSN 0014-3057. Available from: https://doi.org/10.1016/j.eurpolymj.2019.05.005.

38. PENUMADU, Dayakar, Jun-Cheng CHIN, Stephen YOUNG, Frederick IGNATZ-HOOVER, and Tom FLOYD. *Sulfur Dispersion Quantitative Analysis in Elastomeric Tire Formulations by Using High Resolution X-ray Computed Tomography*. Online. Rubber Chemistry and Technology, vol. 94 (2021), no. 4, pp. 626–641. ISSN 0035-9475. Available from: https://doi.org/10.5254/rct.21.79997.
39. LI, Xiangyan, Qiuping YANG, Han LI, Liqun ZHANG, and Song HONG. *Quantifying the 3D multiscale dispersion structure of nanofillers in polymer nanocomposites by combining 3D-STEM and Synchrotron Radiation X-ray CT*. Online. Composites Part B: Engineering, vol. 212 (2021), 108687. ISSN 1359-8368. Available from: https://doi.org/10.1016/j.compositesb.2021.108687.
40. WANG, B., B. PAN, R. TAO, and G. LUBINEAU. Systematic errors in digital volume correlation due to the self-heating effect of a laboratory X-ray CT scanner. *Experimental Mechanics*, vol. 56 (2016), no. 4, pp. 1–12. ISSN 0014-4851.
41. HOLGADO, Ibon, Naiara ORTEGA, José A. YAGÜE-FABRA, Soraya PLAZA, and Herminso VILLARRAGA-GOMEZ. Metrological evaluation and classification of porosity in metal additive manufacturing using X-ray computed tomography. *Materials & Design*, vol. 254 (2025), 114057. ISSN 0264-1275.
42. BAUMGÄRTNER, Benjamin, Richard ROTHFELDER, Sandra GREINER, Christoph BREUNING, Jakob RENNER, et al. *Evaluation of Additively-Manufactured Internal Geometrical Features Using X-ray-Computed Tomography*. Online. Journal of Manufacturing and Materials Processing, vol. 7 (May 2023), no. 3, p. 95. ISSN 2504-4494. Available from: https://doi.org/10.3390/jmmp7030095.